TRACE METALS IN ARCTIC FAST ICE

By

Vincent Domena

A Thesis Submitted in Partial Fulfillment of the Requirements

for the Degree of

Master of Science

in

Oceanography

University of Alaska Fairbanks

December 2017

APPROVED:

Ana Aguilar-Islas, Committee Chair
Robert Rember, Committee Member
Andrew McDonnell, Committee Member
Mark Johnson, Department Chair
Department of Oceanography
S. Bradley Moran, Dean
College of Fisheries and Ocean Sciences
Michael Castellini, *Dean of the Graduate School*

Abstract

Trace metals in the marine environment are found in trace amounts, but are important tracers of oceanographic processes, and bioactive trace metals can impact ocean biogeochemistry through their nutrient or toxic influence of microbial populations. Sea ice is an intrinsic feature of the Arctic Ocean that likely plays a key role in the cycling of trace metals, given that this substrate can concentrate, alter, and transport these elements. Warming conditions in the Arctic have decreased sea ice cover over the past decades and the loss of sea ice threatens to drastically change the Arctic ecosystem, but the implications are not entirely understood. The scarcity of studies on Arctic sea ice entrained trace metals is due in part to the lack of commercially available sampling equipment capable of collecting sea ice without introducing contamination, and in part to the logistic and economic difficulties in accessing remote Arctic sea ice sites. Natural heterogeneity related to large sediment loads incorporated in uneven patches across Arctic fast ice poses a challenge when designing observational studies of trace metals in sea ice. The scope of this thesis is on the study of trace metals in Alaskan Beaufort Sea fast ice environment. The study includes snow, sea ice and seawater under the ice. Analysis of dissolved (Mn, Fe, Cu and Zn) and particulate (Al, Mn, Fe, Cu and Zn) phases was carried out from 50 ice cores collected with a trace metal clean ice corer developed at the University of Alaska Fairbanks. The results of this study indicated that the ice corer developed at UAF was able to collect uncontaminated samples. Highly variable and elevated concentrations of particulate (> 0.2 μm) trace elements were observed due to the notable variability in the amount of sediment incorporated within ice cores, but surprisingly dissolved (< 0.2 μm) metal concentrations were relatively low and consistent. The observed low dissolved metal concentrations, along with low bulk salinity and low percent leachable particulate trace metal fractions, suggest that desalination removed reactive metals from the ice matrix prior to sampling. Spatial variability of dissolved and particulate trace metals was statistically analyzed and indicated generally negligible variability on the meter scale, but significant variability on the kilometer scale, for both size classes. These results emphasize that future studies of trace metals in sea ice should include temporal and spatial considerations.

Table of Contents

List of Figures

Page

List of Tables

Acknowledgements

I would first like to thank my advisor, Dr. Ana Aguilar-Islas for this amazing opportunity, as well as her support and confidence in me throughout my master's. I'd also like to thank Dr. Ana Aguilar-Islas and Dr. Robert Rember for working with me on my journal submission to Marine Chemistry (Chapter 2). Their assistance with sample collection, sample analysis and editing was irreplaceable. I also want to acknowledge my funding sources, Coastal Marine Institute (CMI) through the Bureau of Ocean Energy Management (BOEM), as well as the National Science Foundation (NSF) for the opportunity to pursue this project.

For their help with tasks such as sample collection, sample processing, thesis editing and/or moral support, I'd like to express my gratitude to Mette Kaufmann, Dr. Jeremy Kasper, Dr. Andrew McDonnell and my friends at the University of Alaska Fairbanks (UAF).

Finally, I owe many thanks to my family for everything they have done for me, especially my parents who have always supported me unconditionally, not only in my academics, but also in life.

Chapter 1: Introduction

1.1 Preface

Decreases in Arctic sea ice extent are expected to create more favorable conditions for phytoplankton growth in Arctic waters (Arrigo et al., 2008). However, the change in Arctic biogeochemistry from reduced sea ice is not well understood. Increases to sea ice-related primary production have been observed seasonally in ice-edge blooms in the Arctic (Perrette et al., 2011) and Southern Ocean (Smith and Nelson, 1985), due to increased vertical stability of surface waters from the mixing of fresher meltwater (Smith and Nelson, 1985) and the addition of micronutrients released from melting sea ice (Vancoppenolle et al., 2013). Micronutrients are trace metals in the marine environment, such as iron (Fe), which tend to accumulate in sea ice (Aguilar-Islas et al., 2008). About 7% of the global ocean is covered by sea ice (Perovich et al., 2008) but trace metals in sea ice have rarely been analyzed. Sea ice is an intrinsic feature of high latitude ecosystems, but increasing global temperatures and accompanying climatic changes threaten to drastically change sea ice regimes (IPCC, 2014). Arctic temperatures have increased at an alarming rate, totaling approximately 2°C to 4°C in the last 50 years (Walsh, 2014). Sea ice extent is decreasing in the Arctic (Alekseev et al., 2016; Stroeve et al., 2014), and the potential for sea ice-free summers in the Arctic is projected to occur within this century (IPCC, 2014), completely altering the sea ice regime from being dominated by thick, multi-year ice, to dominated by thinner, one-year ice.

1.2 Seasonal processes in sea ice, sea ice transport and trace metal content of Arctic fast ice

Sea ice formation begins in the fall as the entire mixed layer reaches the freezing point. Tiny crystals called frazil ice then form throughout the water column, some attaching to suspended particles as they float to the surface, and at depths of < 60 m frazil ice can attach to particles on the seafloor (Darby et al., 2011). Frazil ice accumulates at the sea surface, where in calm conditions it congeals into nilas ice and eventually ice sheets. Ice connected to shore or anchored to the seafloor is known as fast ice, typically found in shallow water columns, as opposed to free floating ice, referred to as pack ice, which can form at any depth. In rough conditions, frazil ice at the surface forms into disc shaped ice, referred to as pancake ice, and as pancakes raft together, eventually cement into ice sheets. Typically, the Arctic is dominated by calm conditions but evidence suggests that with receding ice cover, rough conditions will

increase (Perovich et al., 2008). Rougher conditions in the Arctic may lead to further increases of sediment resuspension that could be entrained in sea ice during formation. Enhanced sediment incorporation is especially likely as fall storms in the Arctic intensify (Serreze et al., 2000), and resuspend sediment in shallow Arctic shelves (Eicken et al., 2005). As sea ice continues to grow downward, salt is expelled into surrounding water, increasing the salinity and density of water, which assists to supercool surrounding water as it sinks (Petrich and Eicken, 2009). However, some of this brine may be caught within the ice matrix in compartments known as brine pockets, which harbor dissolved constituents in the brine, including dissolved trace metals (van der Merwe et al., 2011). Brine pockets can also enclose small biological and sedimentary particles that can contribute to trace metal loads within the sea ice (van der Merwe et al., 2011).

After sea ice sheets have formed, exchange at the ice/water interface influences dissolved and particulate trace metal cycling at the base of the sea ice, where the availability of nutrients can result in a thick basal layer of sympagic algae (Arrigo, 2014). Metal cycling between dissolved and particulate phases is also influenced by microbes inhabiting brine pockets throughout the sea ice matrix and/or by abiotic cycling of chemically labile metal species. In addition, snow and dry deposition accumulated on the surface of sea ice increases trace metal concentrations during the melting season. Atmospheric deposition over the Arctic Ocean is primarily from anthropogenic dust originating from mid-latitudes (Bian et al., 2013). The greatest amount of atmospheric deposition is deposited in the early spring and late winter (Breider et al., 2014). Notable sources of aerosols into the Arctic are desert dust (Jickells et al., 2005), anthropogenic particles especially in Arctic Haze (Shaw and Khalil, 1989) and glacial dust (Groot Zwaaftink et al., 2016; Bullard, 2016). Furthermore, in shallow waters sea ice may be thick enough or have a keel that scrapes across the seafloor entraining sediment (Nurnberg et al., 1994), which potentially can be transported away from shallow regions where rafting occurred, thereby influencing trace metal cycling over a broader area.

Solar radiation during spring increases the temperature of the atmosphere and the sea ice environment. The high albedo of snow and ice compared to that of seawater (Dieckmann and Hellmer, 2009) results in slower warming in regions of full sea ice cover relative to marginal ice zones and along leads. The rise in seawater temperature contributes to the warming of ice and to

melting (Curry et al., 1995). As sea ice continues to melt, more seawater is exposed, which warms the Arctic surface ocean further, and promotes sea ice melting; this mechanism is known as ice-albedo feedback (Curry et al., 1995). Eventually sea ice warms to a threshold where brine channels expand, become connected, and and ice becomes permeable allowing for the release of brine via gravity drainage (Golden et al., 2007). Thus along with the brine, the majority of dissolved metals are released into the underlying surface water by the initial desalination after ice becomes permeable (van der Merwe et al., 2011). Sea ice permeability is governed by "the rule of fives" (Golden et al., 1998), which states that for columnar ice the transition from impermeable to permeable ice takes place when the brine volume of sea ice increases to about 5%. This sea ice brine volume is reached when ice temperature is - 5°C for sea ice with a bulk salinity of 5 (Golden et al., 1998). Observations show that once the sea ice hits the threshold, seawater can freely percolate to the surface of the ice and mix with snow, affecting meltpond formation and drainage (Golden et al., 1998). The bulk of ice particles associated with the sea ice matrix are released later than dissolved constituents when the ice matrix melts, and thus the release of particulate trace metals impacts the water column later in the season (van der Merwe et al., 2011). Depending on size and density, and the depth of the water column, particles released from sea ice will exhibit varying residence times within the water column before contributing to sedimentation. Only recently have particulate metals been considered to add to the potentially bioavailable fraction of metals in the water column (Wells et al., 1995). Reactive coatings on particles can exchange to the dissolved phase and particle reactive dissolved metals can absorb onto sinking particles. The longer the residence time, the greater the opportunity for reactions to occur and since particulate metals may take longer to dissolve, sediment released from sea ice has the potential to impact the biogeochemical cycling of trace metals over longer periods than the release of dissolved metals earlier in the season.

Warming during the Arctic spring creates conditions prime for phytoplankton growth (Arrigo, 2014). Initially, recent studies have found that under ice blooms in the Arctic can occur due to thinning sea ice, which allows sufficient light to reach the underlying seawater (Arrigo et al., 2008). Phytoplankton ice edge blooms also occur, but this is as a result of enhanced vertical stability from ice melt and surface warming (Perrette et al., 2011). Traditionally, the Arctic has been seen as a nitrate and light limited system, however co-limitation has been demonstrated in

the Beaufort Sea in late summer (Taylor et al., 2013). With decreases to sea ice caused by global warming, Fe supply by sea ice may be decreased resulting in further Fe limitation/co-limitation (Taylor et al., 2013), but it may be off-set by Fe inputs from atmospheric deposition and increased mixing of the water column (Hoffmann et al., 2012).

Pack ice and fast ice that break away from its anchor point have the ability to transport sea ice entrained constituents away from areas of formation and have broader biogeochemical impacts in Arctic waters (Eicken et al., 2005). However, coastal sea ice mobility is decreased by geological features (e.g., barrier islands) and/or by physical processes that enhance melting before ice can break up and be transported (e.g., river flow in early spring; Kasper and Weingartner, 2015). These impeding factors are more likely to affect nearshore ice, where due to shallow depths, sea ice is likely to contain great sediment loads. Sea ice that is mobile can move at speeds of 6 – 7 km/day (Rampal et al., 2009), and when it melts, it can release its sediment load 100's of kilometers away from the region of formation. Sediment release by melting sea ice within Arctic basins is considered to be a major factor dictating sedimentation rates in the region (Eicken et al., 2005). The potential sediment load in Chukchi Sea sea ice was estimated for the Winter of 2001/2002 to be on average 128 tonnes/km^2, which means sea ice formed on shelves has the potential to transport considerable amounts of sediment to the Arctic basin (Eicken et al., 2005). Melting sea ice is considered to be an important source of particulate and dissolved Fe, as well as other trace metals across the Arctic (Tovar-Sánchez et al., 2010).

Trace metals are incorporated into landfast sea ice directly from the water column (Hassler and Schoemann, 2009), from atmospheric deposition (Lannuzel et al., 2016) and from suspension of sedimentary particles by frazil ice (Darby et al., 2011). In the nearshore, trace metal distributions in the water column can be influenced by river input (Klunder et al., 2012), biological activity and sediment resuspension. There are two studies prior to this thesis of trace metals in Arctic fast ice, one of which analyzed a large suite of particulate trace metals in the Laptev Sea (Holemann et al., 1999) and the other that analyzed particulate Fe near Barrow, AK (Taylor, 2015). There are also limited studies on pack ice, one of which analyzed a suite of trace metals in Fram Strait (Tovar-Sánchez et al., 2010) and another that analyzed a suite of elements in the Canadian Archipelago (Campbell and Yeats, 1982). Utilizing minimal data on trace metals

in Arctic sea ice, there was an attempt to model dFe concentrations in Arctic sea ice (Wang et al., 2014) and according to the authors, this model tends to report lower concentrations of dFe, probably due to underestimating sediment loads in sea ice but there is not enough evidence yet to validate this model.

The limited number of studies on trace metals in sea ice is a result of difficult logistics in accessing Arctic sea ice and the fact that not until recently has custom-made, trace metal clean ice sampling equipment been developed. One such trace metal clean ice corer was used for the ice sampling work described in Chapter 1 of this thesis. This custom-made ice corer was developed at UAF, and is made of ultra-high-molecular-weight polyethylene and commercial-grade titanium. Tests show the corer is clean for several trace metals of interest (data not shown). This ice corer is also fitted with removable low-density polyethylene sleeves which receive the ice core while coring, and is capped immediately after coring to help eliminate contamination during transport of the ice core. Studies of trace metals in sea ice have increased in recent years, such as during Arctic GEOTRACES cruises in 2015. The efforts to analyze trace metals in sea ice come at a time of great change in the Arctic and more data will help to predict how the warming Arctic will impact trace metal inputs to the Arctic Ocean surface waters.

1.3 Changing Arctic

Changes to the Arctic sea ice regime stem from climatic changes which are intensified in the Arctic (Richter-Menge and Mathis, 2016). The Arctic has risen 2°C to 4°C degrees in the past 50 years (Walsh, 2014). Part of this increase in Arctic temperature is also due to the influence of black carbon deposited from the atmosphere onto the sea ice environment, because black carbon inclusions in the sea ice and snow decreases the albedo, which increases the amount of heat absorbed by solar radiation (Liu et al., 2015; Popovicheva et al., 2017). Increasing amounts of black carbon are being deposited in the Arctic from the burning of fossil fuels and other biomass such as forest fires (Popovicheva et al., 2017), which is expected to contribute to future warming. The warmer temperatures in the Arctic have resulted in longer melting seasons (Markus et al., 2009; Stroeve et al., 2014), increased rates of melting sea ice extent over the past 30 years (Comiso et al., 2008) and decreases in Arctic sea ice thickness from 3.64 m in 1980 to 1.85 m in 2008 (Kwok and Rothrock, 2009) with continuing decreases (Kwok and Cunningham,

2015; Laxon et al., 2013). Studies of trace metals in sea ice have increased in recent years, such as during Arctic GEOTRACES cruises in 2015. The efforts to analyze trace metals in sea ice come at a time of great change in the Arctic and more data will help to predict how the warming Arctic will impact trace metal inputs to the Arctic Ocean surface waters.

1.4 About Chapter 2

In Chapter 2 of this thesis, I present first time sea ice trace metal data that includes dissolved and particulate Al, Mn, Fe, Cu and Zn from Beaufort Sea fast ice. Samples were collected ~ 8.5 to 12 km off the coast of Oliktok Pt., AK. An important aspect of this study is the inclusion of methods to determine spatial heterogeneity of trace metal distributions in sea ice that address representative sampling concerns stemming from observations in past studies (e.g. Aguilar-Islas et al., 2008; Tovar-Sanchez et al., 2010; Lannuzel et al., 2010). Sea ice is intrinsic to the Arctic and plays an important role in trace metal biogeochemistry. More data are needed to fully understand how trace metal concentrations vary spatially and seasonally across the Arctic, which will increase modeling capabilities in the future. Chapter 1 of this thesis adds to our understanding of concentrations of dissolved (Mn, Fe, Cu, Zn) and particulate (Al, Mn, Fe, Cu, Zn) trace metals in Arctic fast ice and the spatial heterogeneity of these trace metal concentrations in this dynamic environment.

Chapter 2: Spatial variability of Al, Mn, Fe, Cu and Zn in Beaufort Sea fast ice[1]

2.1 Abstract

The cycling of trace metals in sea ice plays an important role in the biogeochemistry of polar oceans, yet little is known about trace metals in Arctic sea ice. The Arctic Ocean is a sensitive ecosystem impacted by anthropogenic inputs such as oil exploration and industry, which can contaminate natural trace metal concentrations in the environment. Areas of Arctic fast ice formation are close to land which is a source of natural and anthropogenic inputs of trace metals to the nearshore environment. Unevenly distributed visible inclusions of sediment have been observed in fast ice formed over Arctic shelves making this environment naturally heterogeneous. In this study first time data of dissolved (Mn, Fe, Cu and Zn) and particulate (Al, Mn, Fe, Cu and Zn) trace metals was generated from Alaska Beaufort Sea fast ice to assess the variability of trace metal distributions in this dynamic environment. Trace metal to Al ratios from sea ice particles show no evidence of anthropogenic contamination and based on these ratios, sediment is mainly lithogenic. The low bulk salinity and dissolved metal concentrations in the sampled sea ice along with low percent leachable particulate metal fractions suggest that desalination had removed reactive metals from the sea ice matrix prior to sampling. Statistical analysis of the dissolved and particulate trace metal data indicated generally negligible variability intra-station (meter scale) but significant variability inter-station (kilometer scale). Based on the results of this study future sampling of trace metals in Arctic fast ice should include temporal variability and focus on kilometer-scale spatial variability.

2.2 Introduction

Sea ice dynamics affect trace metal cycling in polar waters (Vancoppenolle et al., 2013). Sea ice studies have demonstrated enhancement of dissolved (< 0.2 μm) and particulate (> 0.2 μm) trace metal concentrations in sea ice compared to the underlying seawater (e.g. Holemann et al., 1999, Aguilar-Islas et al., 2008; Lannuzel et al., 2014). Dissolved metals (dMetals) are retained in brine pockets created during ice formation; these may also contain particles. Suspended particles in the freezing surface layer can be trapped in the ice matrix contributing to

[1] V. Domena, R. Rember, A. Aguilar-Islas
Document prepared for submission to Marine Chemistry

sea ice particulate metal (PMetal) loads and, in water depths of < 60 m, frazil ice adhesion on seafloor sediment can assist in suspending more particles to the base of sea ice (Darby et al., 2011). These processes create a substrate with heterogeneous trace metal distribution.

Heterogeneity is further enhanced after sea ice has formed by processes such as exchange with seawater at the base of sea ice (basal ice), atmospheric deposition on the sea ice (Edwards and Sedwick, 2001), the rafting of ice floes onto one another (Kempema et al., 1989), and entrainment of particles by ice keels dragging across the seafloor (Nurnberg et al., 1994). Sediment incorporated into sea ice can experience large-scale transport. For example, it was estimated that in 2001/2002 Arctic sea ice formed across the Chukchi Sea and Beaufort Sea shelves was responsible for transporting 5×10^6 to 8×10^6 tonnes (t) of sediment from the shelf to the Arctic basin (Eicken et al., 2005). In other cases, coastal sea ice may not move far from its area of formation if it is geographically contained, such as by islands, or when landfast ice melts readily post break-up by coastal processes such as river input (Kasper and Weingartner, 2015).

During the melting season snow melt transfers dissolved and particulate metals accumulated from atmospheric deposition into the sea ice. Sea ice brine pockets begin to expand as temperatures increase, creating a network of brine channels that release brine when sea ice becomes permeable. The transition from impermeable to permeable conditions occurs at a brine volume fraction of ~ 5%, which happens when temperature increases to – 5°C for an ice column with a typical bulk salinity of 5 (Cox and Weeks, 1983; Golden et al., 1998). This is known as the "rule of fives." Dissolved metals are initially released when sea ice becomes permeable (van der Merwe et al., 2011), while particles are mainly transferred to the water column at a later time, after the ice matrix begins melting (van der Merwe et al., 2011). In addition to sea ice as a source of trace metals to the Arctic water column, studies on Arctic shelves of Alaska suggest elevated concentrations of trace metals in the water column can be influenced by river input (Cid et al., 2012; Klunder et al., 2012), enhanced mixing by bathymetric features such as Barrow Canyon (Aguilar-Islas et al., 2013), and by snow melt from land (Rember and Trefry, 2004). Sediment studies have shown little to no anthropogenic influence on trace metal concentrations even in Arctic oil drilling areas (Trefry et al., 2003). Although sea ice is an intrinsic feature of the Arctic Ocean and trace metal cycling can potentially alter the Arctic Ocean ecosystem,

published data on trace metal concentrations in Arctic sea ice is limited (Aguilar-Islas et al., 2008; Campbell and Yeats, 1982; Granskog and Virkanen, 2001; Holemann et al., 1999; Kanna et al., 2014; Tovar-Sánchez et al., 2010; Taylor, 2015), with the majority of recent studies being constrained to the subarctic.

The dearth of trace metal data in sea ice is in part a result of the lack of commercially available trace metal clean sampling and processing equipment, and logistical difficulty in accessing Arctic sea ice. Prior studies that relied on commercially available equipment have had to include laborious post-collection cleaning processes (e.g., Aguilar-Islas et al., 2008; Tovar-Sánchez et al., 2010). Other studies have been carried out with the use of expensive, custom-made sampling equipment (e.g., Lannuzel et al., 2014; van der Merwe et al., 2011). Here we present trace metal data from sea ice collected at the North Slope of Alaska that include first time data for Al, Mn, Fe, Cu and Zn from nearshore fast ice in the western Beaufort Sea. Statistical analysis was used to determine the heterogeneity of dissolved and particulate trace metals, within and among sampling sites.

2.3 Methods

2.3.1 Study Site and Sampling

Samples were collected 16 -17 May 2015 from five sites east of the Colville River and north of Oliktok Point, Alaska (Fig. 1). Sampling took place within a 30 km^2 area that is impacted annually by the Colville River outflow. Although the area sampled was flooded with river water on 19 May, evidence of river flow was not observed during the May 16 - 17 sampling. Samples collected at each station consisted of ten 1 m ice cores, one snow sample, and seawater samples from one or two depths under the ice. Cores were stored frozen (-20 °C) after collection in capped pre-cleaned plastic sleeves, and were shipped to the University of Alaska Fairbanks (UAF) for processing. Snow and seawater samples were processed in the field and shipped back to UAF for analysis.

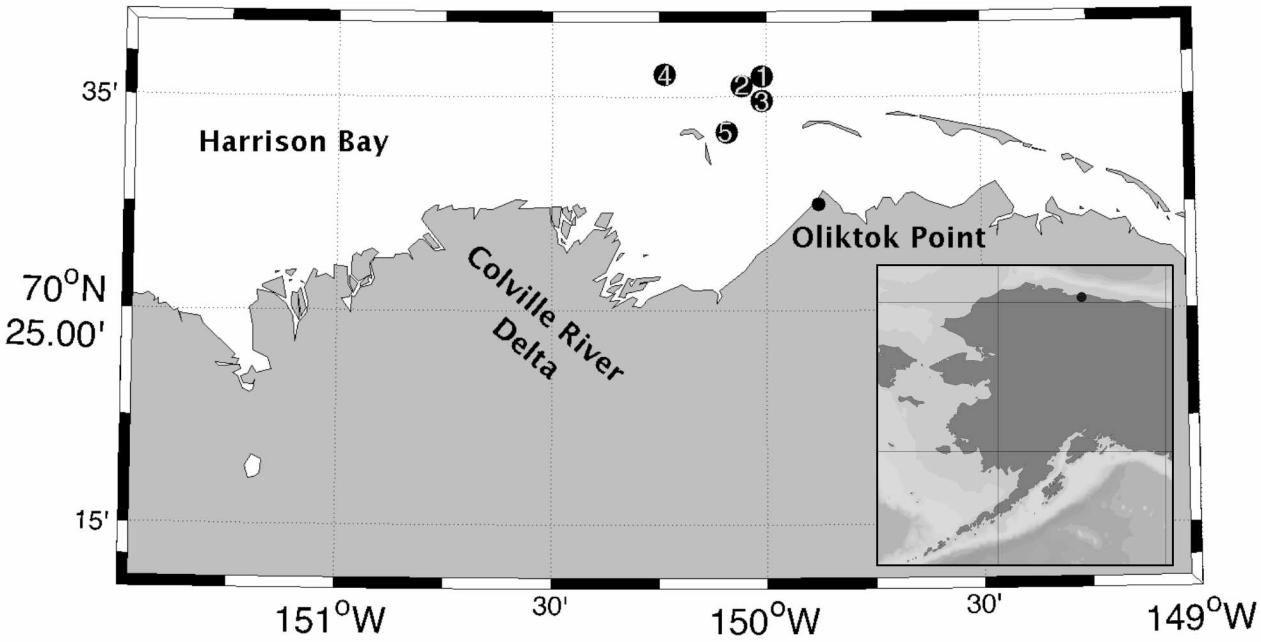

Figure 1: Map of sampling location (Stations 1 through 5) in the vicinity of barrier islands just north of Oliktok Point, AK. Inset: Oliktok Point location on State of Alaska map.

Collection of ice cores was done cleanly using a trace metal clean ice corer developed at UAF (Fig. 2). The corer is 1 m in length, with a shaft comprised of two UHMW polyethylene tubes, joined together by a ring of commercial grade titanium (CP2). The shoe and cutting blades are made of the same grade titanium. Titanium rather than stainless steel was used to avoid potential contamination of metals of interest. Additionally, this device incorporates a removable low density polyethylene (LDPE) shaft insert (sleeve) that receives the ice core as it is being drilled, and is then capped at both ends once removed from the corer shaft with fitted plastic caps further secured to the outside of the sleeve with electrical tape. This minimizes contamination post coring and during transport. The core collection scheme employed consisted of five cores collected within a 1 m^2 area (grouped cores) and additional five cores randomly collected within 10 m^2 peripheral area (random cores) (Fig. 3).

Snow was collected directly into cleaned 1 L wide-mouth LDPE bottles. Sample bottles were double-bagged and transported at the end of the day to a makeshift field lab, where they were melted. The resulting small volumes of melted snow precluded filtration, as insufficient volume was available to rinse the filtration apparatus and sample bottle. Thus only unfiltered

snow melt was processed for analysis. Seawater from under the ice was collected using a rotary pump (IWAKI magnetic drive pump, model WMD-30LFY-115) with plastic wetted parts connected to Teflon-lined tygon tubing (1/2" ID, Cole Parmer). Prior to collection a hole was drilled with an ice auger and an ice tent was erected over the hole, and the area was left undisturbed for at least 1 hour while snow and ice collection were completed. The waiting time allowed water potentially contaminated during drilling to flow out of the area and to be replaced by unperturbed ambient seawater. Unfiltered samples were collected into pre-cleaned 500 ml LDPE bottles, double bagged and transported to the makeshift lab for processing. The makeshift lab consisted of a plastic enclosure constructed on top of a table; a HEPA filter unit (Envirco Corporation) was used to maintain positive pressure inside the enclosure. A custom vacuum filtration system was used to filter the samples through pre-cleaned 47 mm filters (0.4 µm, Nucleopore track etched polycarbonate (PC)) and received in pre-cleaned 100 mL LDPE sample bottles. Unfiltered snow samples, filtered and unfiltered seawater samples were double bagged and transported back to UAF for acidification and analysis.

Figure 2: Components of trace metal clean ice corer developed to collect 1 m ice cores for this study. On the left is the connector to the battery powered drill. In the middle is the barrel of the corer made of ultra-high-molecular-weight plastic connected by a titanium joint, and terminated with titanium cutting part. On the right is the removable low density polyethylene sleeve, which is inserted into the corer to receive the ice during coring.

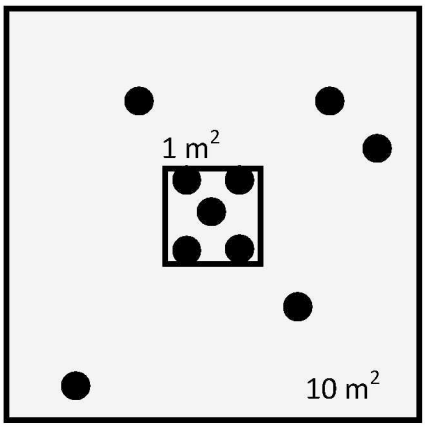

Figure 3: Ice core sampling scheme (not to scale) carried out at each station to assess intra-station variability of trace metal concentrations. 5 ice cores taken within 1 m^2 box (grouped cores) and 5 cores taken randomly (random cores) within 10 m^2 of the grouped cores.

2.3.2 Cleaning protocols

Sampling devices, filters, and plasticware were cleaned with a dilute soapy solution (micro-90, Cole Parmer), and three sequential acid steps (10% v/v reagent grade (RG) hydrochloric acid (HCl), 0.1% v/v trace metal grade (TMG) HCl, and 0.1% v/v TMG HCl). Overnight heating (60 °C) and copious rinsing with ultra-high purity water (UHP water, Milli-Q®) took place after each step. Polyethersulfone (PES) Supor® filters (0.2 µm pore size) and PC Nucleopore filters were cleaned and stored in Teflon jars (Savillex). For Supor® filters the side facing up in the package is recommended by the manufacturer to be used as the upstream side for better flow, but it is difficult to determine the top from the bottom once the filters are removed from their original box, so attention is needed to maintain filter direction throughout cleaning and processing. Acid solutions were carefully drained from the container after each step and the filters were then soaked and rinsed multiple times until the pH of the rinse water was that of UHP water.

Plasticware used during processing were cleaned in between samples to prevent cross-contamination. The filtration apparatus used in the field was cleaned between samples with ~ 100 ml of pH < 2 UHP water, and rinsed 3 times with UHP water and rinsed 1x with sample. Similarly, custom-made ice melting chambers were filled with pH < 2 UHP water, heated overnight, and rinsed 3 times with UHP water. Filter holders were cleaned between samples by soaking them in a room temperature acid bath (1% v/v TMG HCl) overnight and rinsing with ultra-high purity water.

2.3.3 Sample processing

Melted snow and seawater samples were acidified to pH < 2 with Optima-grade HCl (Fisher Scientific) in a laminar flow hood (ISO-5) at UAF. Ice cores were processed under HEPA air at UAF's International Arctic Research Center (IARC). The ice cores were individually melted in cleaned custom-made high density polyethylene (HDPE) chambers fitted with a gas inlet at the top of the chamber (Fig. 4). Ultra-pure Argon gas was used to pressurize the chamber (5 to 10 psi) during filtration. The chambers consist of 1 m hollow HDPE cylinders threaded on either end for HDPE caps. The top cap was removed to transfer ice cores from their transport sleeves into the chambers, and re-capped. The base of the bottom cap was fitted with a Teflon 2-way valve (Chemfluoro, ¼ ") connected with Teflon tubing (¼ ") to a 90 mm Teflon filter holder (Savillex), which housed a pre-weighed 90 mm Supor® filter. Ice cores were allowed to melt either overnight at room temperature or over ~ 8 hours with heating tape wrapped outside the chamber. Filtration took place after the ice core was completely melted. The melted sample was homogenized with gentle shaking of melting chamber. The initial ~ 1.5 L of sample were allowed to pass through the filter assembly prior to sample collection into LDPE bottles (500 mL), samples were acidified to pH < 2 with Optima HCl. Procedural blanks were collected in the same manner using UHP water passed through blank filter membranes. Filters were dried overnight on a clean plastic grid in a laminar flow hood (ISO-5) and weighed again once dry. Dry blank and sample filters were cut into fourths on top of a clean plastic cutting board using a rotary cutter fitted with a pre-cleaned blade (50% Optima grade Methanol).

Figure 4: High density polyethylene custom-made melting chambers developed for this study. A gas inlet at the top is used to presurized the chamber with ultra pure gas (Ar or N_2) during filtration, and a valve at the bottom connected to the filter holder with teflon tubing is used to regulate the flow.

2.3.4 Particle leaching procedure

One quarter of the filter was leached with acetic acid after Berger et al. (2008) to determine leachable particulate (LP) metal fractions. We modified the Berger et al. (2008) method by including a centrifugation step. The filter subsample was folded 4 times and transferred to a 2 mL vial. A solution of 25% acetic acid (Aristar® Ultra) with 0.02 M hydroxylamine hydrochloride (1 ml) was added to the folded filter subsample, heated (~ 95°C) in a water bath for 10 minutes, and allowed to cool for an additional 110 minutes. After cooling, vials were centrifuged, and the leachate was carefully transferred to a 10 mL Teflon beaker. Five aliquots of 0.5 mL UHP water used to rinse the filter and vial were transferred to the beaker, with centrifugation in between each rinsing step. Leached filters were kept refrigerated for later digestion. The leachate was dried on a hot plate (~ 80°C). Dried samples were taken up into 150 µL of distilled nitric acid, heated for ~ 2 minutes and transferred to a clean 7 mL polypropylene scintillation vial. The beaker was sequentially rinsed with 1 N distilled HNO_3 and UHP water to create a 4 mL, 5% nitric solution.

2.3.5 Particle digestion procedure

Leached filters were sequentially digested according to digestion D2 detailed in Ohnemus et al. (2014), to determine the refractory particulate (RP) metal fraction. The leached filters were digested using Ultra Grade (Aristar®) hydrofluoric acid (HF), distilled HNO_3 and distilled HCl. Briefly, samples were subjected to distilled HNO_3 (67% v/v) and distilled HCl (33% v/v) overnight at 130°C in tightly capped 15 mL digestion vials (Savillex). A subsequent digestion followed with distilled HNO_3 (62.5% v/v), distilled HCl (31.25% v/v), and concentrated HF (6.25% v/v) at 130°C overnight. In between steps, samples were cooled and then dried at 90°C, and care was taken while opening the vials to prevent losing any sample that may have accumulated near the vial opening. Digestion of samples with a large large sediment load required increased volume of the acid solution with a larger percentage of HF (distilled HNO3: 57.14% v/v, distilled HCl: 28.57% v/v, HF: 14.28% v/v). After the 2nd digestion step, samples were taken up into 1 mL distilled HNO_3, heated for 30 minutes in its capped vial at 90°C, then transferred to a pre-weighed LDPE bottle. The vial was rinsed 4 times with pH < 2 HNO_3 (for a total of 19 ml) and added to the sample to make a 5% nitric solution. Blanks and certified reference materials (CRMs; National Research Council Canada), MESS-3 (Beaufort Sea) and

HISS-1 (Hibernia Shelf), were digested in a similar fashion. We used CRM masses to match our samples (20 to 70 mg); these masses are below the certified amount (250 mg), but have been shown to include representative certified values (Ohnemus et al., 2014).

2.3.6 Analytical methods

Samples were analyzed by inductively coupled plasma-mass spectrometry (ICP-MS, Thermo Finnigan Element 2) at UAF's IARC. Concentrations of trace metals in leachates, digested samples and CRMs were determined using standard curves with In as an internal standard. CRM recoveries are found in Table 1. Dissolved metals in sea ice, snow and sea water were analyzed by isotope dilution (Fe, Cu, Zn) and with the use of a standard curve (Mn; sea ice only) employing an inline seaFast S2 system (Elemental Scientific) after Lagerstrom et al. (2013).

Table 1: Certified Reference Material Values and Recoveries.

Element	MESS-3* (mg/kg)	Certified value (mg/kg)	Percent Recovery	HISS-1* (mg/kg)	Certified value (mg/kg)	Percent Recovery
Al	71,086 ± 3840	85,900 ± 2300	82.8%	5870 ± 537	7300 ± 500	80.4%
Mn	259 ± 0.8	324 ± 12	80%	50.73 ± 3.07	66.1 ± 4.2	76.8%
Fe	37,000 ± 1860	43,400 ± 1100	85.3%	2,190 ± 120	2500 ± 100	87.6%
Cu	28.1 ± 0.9	33.9 ± 1.6	82.9%	2.27 ± 0.7	2.3 ± 0.4	98.7%
Zn	117 ± 2.9	159 ± 8	73.6%	5.5 ± 3.7	4.9 ± 0.8	100%

*n = 3

2.3.7 Statistical Analysis

To determine spatial heterogeneity, the variability in metal concentrations was determined using a two sample F-test and a two-tailed t-test. For individual stations grouped cores and random cores were considered separate populations. To assess heterogeneity at larger spatial scales, all cores from a given station were considered one population and compared to a second population comprised of all ice cores from the other 4 stations. Bulk sea ice dissolved metal concentrations were normally distributed. However, bulk sea ice particulate metal concentrations were not, thus these were log transformed. After determining equal/unequal variance in the populations (F-test) a two-tailed t-test, modified for the appropriate variance was carried out.

2.4 Results

Stations were located 8.5 to 17.4 km from shore in water column depths shallower than 11 m. Snow depths (0 to 60 cm) and sea ice thicknesses (1 to 2 m) were variable among stations. Other station metadata can be found in Table 2. Areas with pressure ridges were present throughout the sampling region and sea ice sediment inclusions were visually evident at all stations. Strong winds up to 21 m/s preceded sampling days. Air temperature on sampling days was between -3°C to 0°C, with a cloud cover < 30% and wind speeds less than 10 m/s. The Colville River began flowing ~ May 15th with peak discharge during May 19th, just 2 days after our sampling was completed. In 2015 the Colville River spring flow occurred earlier and was more voluminous during peak discharge than the previous 12 years (Fig. 5; modified from Kasper and Weingartner, 2015).

Table 2: Station Metadata.

Stn #	Sampling date	Latitude	Longitude	Cloud cover	Water depth	Ice thickness
1	May 16, 2015	70° 34.823	150° 0.603	0%	9.2 m	1 to 1.5 m
2	May 16, 2015	70° 35.949	150° 0.623	~ 5%	9.5 m	1.9 m
3	May 16, 2015	70° 35.505	150° 3.468	~ 10%	9.5 m	1.8 m
4	May 17, 2015	70° 36.080	150° 14.211	~ 60%	10.9 m	1.7 m
5	May 17, 2015	70° 33.345	150° 5.502	~ 30%	5.9 m	1.7 m

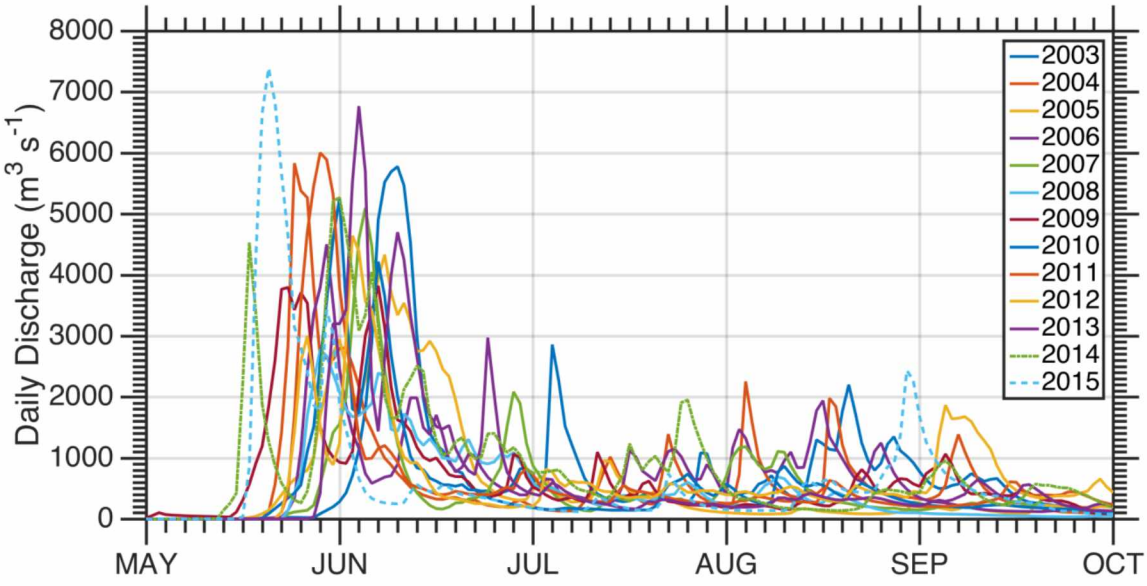

Figure 5: USGS mean daily discharge of the Colville River (2003 – 2015) updated from figure 1 of Kasper and Weingartner (2015). The Colville River had begun to flow by sampling dates, May 16-17, 2015, but it had not yet reached its peak for 2015. No evidence of river water was observed at sampling stations during collection.

2.4.1 Metal fraction definitions

Metals considered part of the reactive pool include metals found in the dissolved phase (0.2 µm filtered sample) (dMetal) and metals readily leached metals from particles. The reactive metal pool was operationally determined either as "total dissolvable metal" (TdMetal), a single value obtained from an unfiltered sample acidified to < 2 pH for > 1 month, which includes dMetals and acid-labile particulate metals (ALP = [TdMetal] – [dMetal]); or from the sum of dMetal concentrations and leachable particulate metals (LPMetals) obtained by treating particles with a 25% acetic acid solution (see Methods section). Metals not leached from particles by the above two methods are considered refractory (RPMetal). These are determined by strong acid digestion of previously leached particles. The sum of LPMetals + RPMetals is considered the total particulate metal (TPMetal) fraction.

2.4.2 Water column data

Reactive metal concentrations in the water column are listed in Table 3. Surface water (~ 2 m depth) was sampled at all stations, with a subsurface sample (> 5 m) at Stations 1, 4 and 5. Concentrations of dFe exhibited a large range (2.76 to 11.47 nM), whereas dCu (5.52 to 6.02 nM) and dZn (2.86 to 4.24 nM) did not. In general, subsurface values were greater for dFe and dZn, but dCu did not exhibit subsurface increases (Table 3). Replicate analysis was done for a

Table 3: Concentrations (nM) of Reactive Metals in the Water Column. Total dissolvable metal (TdMetal) = dissolved metal (dMetal) + acid labile particulate metal (ALPMetal).

Stn	Depth (m)	TdFe (nM)	dFe (nM)	ALPFe (nM)	TdCu (nM)	dCu (nM)	ALPCu (nM)	TdZn (nM)	dZn (nM)	ALPZn (nM)
1	2	48.89	2.86 ± 0.008*	46.03	5.78	5.69 ± 0.08*	0.09	4.23	3.630 ± 0.003*	0.60
	9	191	4.74	186.2	5.95	5.52	0.43	4.23	4.00	0.23
2	2	90.04	4.00	86.04	5.56	5.56	n.d.	3.44	3.39	0.05
3	2	79.92	3.14	76.78	5.90	5.80	0.10	3.51	3.37	0.14
4	2	38.61	2.76 ± 0.02*	35.85	5.62	5.61 ± 0.03*	0.01	2.87	2.86 ± 0.03*	0.01
	9	159.3	6.47	152.84	6.02	6.02	n.d.	4.29	4.24	0.05
5	2	290.5	6.03	284.47	5.85	5.85	n.d.	3.94	3.55	0.39
	5	712.4	11.47 ± 0.005*	700.93	6.00	5.74 ± 0.04*	0.26	4.60	4.02 ± 0.02*	0.58

* n=2; n.d. = non-detectable

subset of samples with excellent analytical agreement of less than 1.5% RSD for all metals. The ALPFe (35.85 to 700.93 nM) was one to two orders of magnitude greater than the dFe fraction, while ALPZn (0.01 to 0.6 nM) and ALPCu (non-detectable (n.d.) to 0.4 nM) concentrations were in general one to two orders of magnitude lower than their dissolved concentrations. Similar to dFe, surface ALPFe was highly variable and was found at greater concentrations in the subsurface. However, unlike ALPFe, concentrations of ALPCu and ALPZn did not follow a trend with depth and were decoupled from dCu and dZn. Analytical agreement in the replicate analysis was variable among elements (ALPFe: 0.14% RSD, ALPCu: 2.3% RSD, ALPZn: 13% RSD).

2.4.3 Snow data

Total dissolvable metal values in snow are listed in Table 4. Similar to the water column, concentrations of TdFe in the snow were more variable and exhibited higher values as compared to concentrations of TdCu or TdZn.

Table 4: Total Dissolvable Metal (TdMetal) Concentrations (nM) in Snow.

Station	TdFe (nM)	TdCu (nM)	TdZn (nM)
1	77.2	0.23	1.09
2	108.7	0.53	3.36
3	26.6	0.46	1.86
4	63.6	0.18	0.94
5	26.8	1.97	0.92
Average	60.6 ± 34.5	0.67 ± 0.74	1.63 ± 1.04

2.4.4 Ice core data

2.4.4a Physical characteristics

Measurements of bulk salinity, ice core volume and the mass of entrained sediment in ice cores are found in Table 5. Core bulk salinity and melted volume exhibited little variability, with an average bulk salinity of 3.6 ± 0.7 and an average volume of 4.3 ± 0.5 L. The mass of entrained sediment per core (or per L of melted sea ice) was highly variable with no apparent trend within or among stations. The average entrained sediment mass was 161 ± 163 mg/core or 36.5 ± 37.0 mg/L.

Table 5: Ice Core Metadata.

Core ID	Bulk salinity	Particle sample wt. (mg)	Melted ice core volume (L)	mg sediment/L
1 grouped-a	3.7	7	5.20	1.35
1 grouped-b	5.1	8	4.54	1.76
1 grouped-c	2.0	7	3.67	1.91
1 grouped-d	2.2	389	4.53	85.97
1 grouped-e	5.0	8	3.11	2.57
Grouped average	3.6 ± 1.5	83.8 ± 170.6	4.2 ± 0.82	18.7 ± 37.6
1 random-a	4.2	19	3.45	5.52
1 random-b	4.8	39	3.73	10.47
1 random-c	4.3	41	4.18	9.82
1 random-d	3.4	147	4.52	32.52
1 random-e	4.4	14	4.36	3.21
Random average	4.2 ± 0.5	52 ± 54.4	4 ± 0.4	12.3 ± 11.7
2 grouped-a	4.1	784	4.50	174.42
2 grouped-b	4.0	178	4.89	36.40
2 grouped-c	2.7	282	3.10	90.97
2 grouped-d	3.4	365	4.25	85.88
2 grouped-e	3.2	134	4.08	1.47
Grouped average	3.5 ± 0.6	323 ± 290	4.2 ± 0.67	77.8 ± 65.4
2 random-a	3.7	566	5.41	104.72
2 random-b	2.6	368	4.37	84.21
2 random-c	3.6	244	4.29	56.94
2 random-d	5.0	180	4.31	41.81
2 random-e	3.5	258	4.01	64.34
Random average	3.7 ± 0.9	323 ± 151	4.5 ± 0.54	70.4 ± 24.5
3 grouped-a	3.3	69	4.81	14.35
3 grouped-b	3.3	234	4.80	48.75
3 grouped-c	3.7	131	4.24	30.90
3 grouped-d	3.5	177	4.84	36.57
3 grouped-e	4.5	178	4.64	38.36
Grouped average	3.7 ± 0.5	158 ± 61	4.7 ± 0.25	33.8 ± 12.6
3 random-a	2.6	163	4.34	37.56
3 random-b	2.9	19	4.36	4.36
3 random-c	4.7	604	4.38	138.06
3 random-d	3.4	184	4.25	43.29
3 random-e	3.2	96	4.03	23.82
Random average	3.4 ± 0.8	213 ± 228	4.3 ± 0.14	49.4 ± 51.8
4 grouped-a	3.9	93	4.75	19.58
4 grouped-b	3.3	170	3.27	52.07
4 grouped-c	2.8	113	5.04	22.44
4 grouped-d	2.8	111	4.33	25.66
4 grouped-e	2.8	279	4.20	66.43
Grouped average	3.1 ± 0.5	153 ± 76	4.3 ± 0.68	37.2 ± 20.8
4 random-a	4.3	159	3.72	42.74
4 random-b	4.3	186	5.02	37.09
4 random-c	3.2	158	4.61	34.31
4 random-d	4.1	194	4.68	41.50
4 random-e	4.3	273	3.95	69.11
Random average	4.0 ± 0.5	194 ± 47	4.4 ± 0.54	45 ± 13.9
5 grouped-a	3.6	30	5.07	5.92
5 grouped-b	3.7	12	4.18	2.87
5 grouped-c	2.5	33	4.36	7.57
5 grouped-d	2.9	8	3.84	2.08
5 grouped-e	3.8	69	4.34	15.90
Grouped average	3.3 ± 0.6	30.4 ± 24.2	4.4 ± 0.45	6.9 ± 5.5
5 random-a	3.9	56	4.39	12.77
5 random-b	3.3	26	3.30	7.88
5 random-c	3.1	49	4.29	11.42
5 random-d	3.1	29	4.14	7.00
5 random-e	4.2	119	4.46	26.71
Random average	3.5 ± 0.5	55.8 ± 36.6	4.1 ± 0.47	13.2 ± 7.95
Average of all	3.6 ± 0.7	161 ± 163	4.3 ± 0.5	36.5 ± 37.0

2.4.4b Dissolved metals

Bulk sea ice dissolved metals are plotted in Figure 6. Manganese had the highest average dissolved concentration (5278 ± 1482 ng/core) and the lowest relative standard deviation among

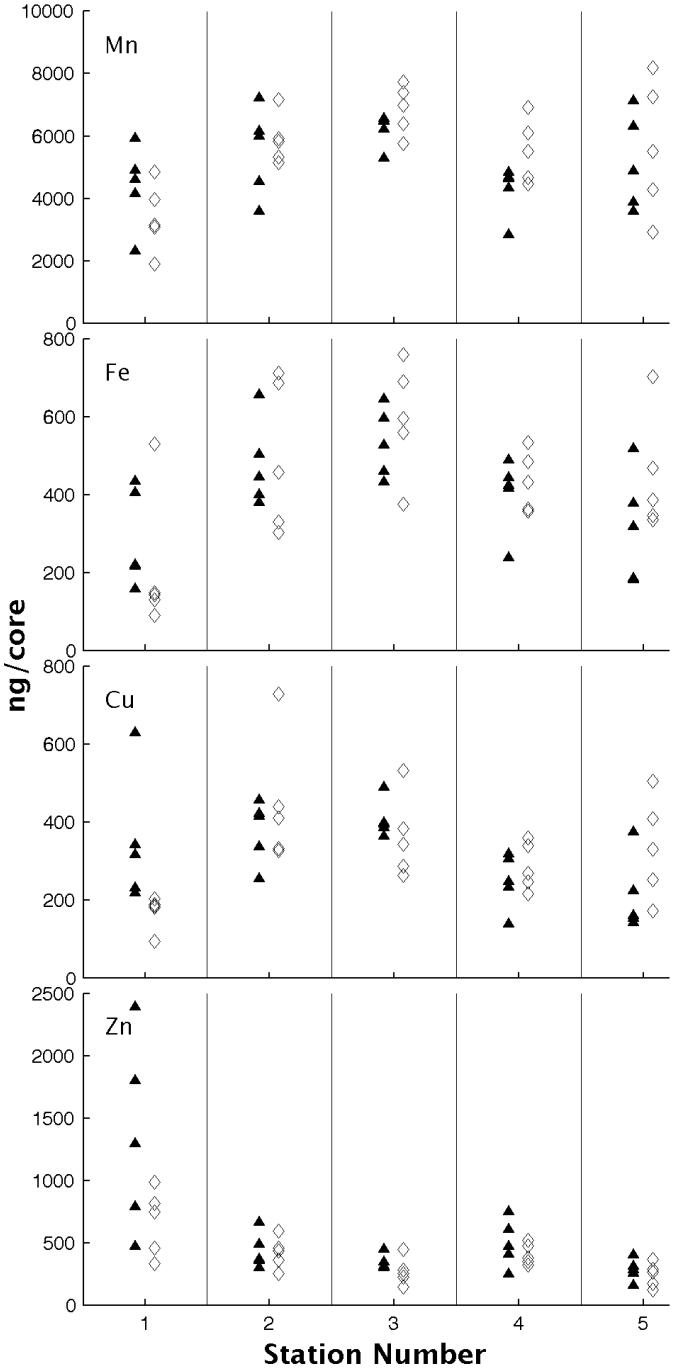

Figure 6: Range of concentrations (ng/core) of dissolved trace elements per 1 m ice core by station (filled triangles: grouped cores; unfilled diamonds: random cores). Values for dissolved Zn at Station 1 are suspected of contamination.

cores compared to the other trace metals analyzed. The concentration of dMn was largest at Station 5 and least at Station 3. Concentrations of dFe were on average 418 ± 167 ng/core (Fig. 6b). Unlike dMn, the concentration of dFe was highly variable, ranging from 90 to 759 ng/core. The average dCu concentration in ice cores was 319 ± 127 ng/core (Fig. 6c). The greatest concentration was found at Station 2, and the lowest concentration at Station 1. Bulk sea ice dZn concentrations had an average of 491 ± 402 ng/core with the highest relative standard deviation among all dMetals, likely driven by high variability at Station 1 where dZn ranged from 332 to 2389 ng/core (Fig. 6d). We suspect potential dZn contamination from the corer during its initial use at Station 1. The concentration range and the average concentration are lower when Station 1 is removed, 332 to 748 ng/core and 361 ± 138 ng/core, respectively. Despite the high variability seen amongst cores there were no significant differences within stations, but there were significant differences for comparisons of one station to all others (Table 6).

Table 6: Statistical Results for Sea Ice Dissolved Trace Metals. p values from t-test comparisons (α= 0.05) within and amongst stations.

Comparison	dMn	dFe	dCu	dZn
Stn 1 g vs. r	0.23	0.45	0.06	0.12
Stn 2 g vs. r	0.61	0.83	0.41	0.86
Stn 3 g vs r	0.18	0.42	0.42	0.24
Stn 4 g vs r	0.06	0.57	0.39	0.38
Stn 5 g vs r	0.69	0.11	0.12	0.54
Stn 1 vs all	0.07	1.3E-4*	0.09	0.01*
Stn 2 vs all	0.28	0.14	0.009*	0.33 (0.04*)
Stn 3 vs all	2.2E-4*	0.001*	0.07	0.003* (0.06)
Stn 4 vs all	0.002*	1.0	0.04*	0.57 (0.01*)
Stn 5 vs all	0.57	0.34	0.20	2.9E-4* (4E-3*)

Grouped cores (g), randomly collected cores (r). * indicated statistical difference ($\leq$ 0.05); values in parentheses exclude station 1.

2.4.4c Particulate metals

Figure 7 displays the TPMetal trace element concentrations (ng/core) for Al, Mn, Fe, Cu and Zn by station. The range of metal concentrations in order of abundance were TPAl ($4x10^4$ to $2.2x10^7$ ng/core), TPFe ($1.75x10^4$ to $1.19x10^7$ ng/core), TPMn (165 to $2.34x10^5$ ng/core), TPZn (11.89 to $1.43x10^4$ ng/core) and TPCu (1.76 to $9.49x10^3$ ng/core). Element concentrations varied by as much as 3 orders of magnitude. The large variability reflects heterogeneity in entrained

sediment. In general, for all TPMetals, statistical differences were not apparent in grouped vs random populations at a given station, but there were significant differences between one station vs all other ice cores (Table 7).

Table 7: Statistical Results for Sea Ice Particulate Trace Metals. p value results from t-test comparisons (α= 0.05) of within and amongst stations.

Comparison	TPAl	TPMn	TPFe	TPCu
Stn 1 g vs. r	0.75	0.06	0.75	0.77
Stn 2 g vs. r	0.17	0.29	0.18	0.20
Stn 3 g vs r	0.17	0.06	0.19	0.24
Stn 4 g vs r	0.01*	0.058	0.08	0.04*
Stn 5 g vs r	0.02*	0.02*	0.02*	0.08
Stn 1 vs all	1.53E-9*	8.8E-9*	1.9E-9*	1.1E-4*
Stn 2 vs all	1.06E-6*	6.4E-8*	8.2E-7*	1.8E-6*
Stn 3 vs all	0.02*	0.05*	0.02*	9.2E-3*
Stn 4 vs all	3.6E-5*	2.6E-4*	3.5E-5*	9.7E-5*
Stn 5 vs all	0.12	0.02*	0.04*	0.19

Grouped cores (g), randomly collected cores (r). * indicated statistical difference ($\leq$ 0.05)

Figures 8 and 9 show values for Al, Mn, Fe, Cu and Zn in LPMetal and RPMetal pools, respectively. The LPMetal concentrations ranged from 442 to $1.26x10^5$ ng/core for Al, 69 to $1.67x10^5$ ng/core for Mn, $2.11x10^3$ to $2.42x10^6$ ng/core for Fe, 1.34 to $4.44x10^3$ ng/core for Cu, and 4.4 to $5.46x10^3$ ng/core for Zn. Concentrations of RPMetals were at least 1 order of magnitude greater than LPMetals for Al and Fe, whereas for Mn, Cu and Zn leachable and refractory fractions were within the same magnitude. The percentage of metals that were leachable in particles ([LPMetal]/[TPMetal]*100) followed an expected trend, with Al exhibiting the lowest percentage (0.43% ± 0.86%), Mn (30.5% ± 18.1%) and Zn (32.2% ± 20.44%) the highest percentage, and Fe (7.7% ± 9.9%) and Cu (18.8% ± 15.7%) with intermediate values.

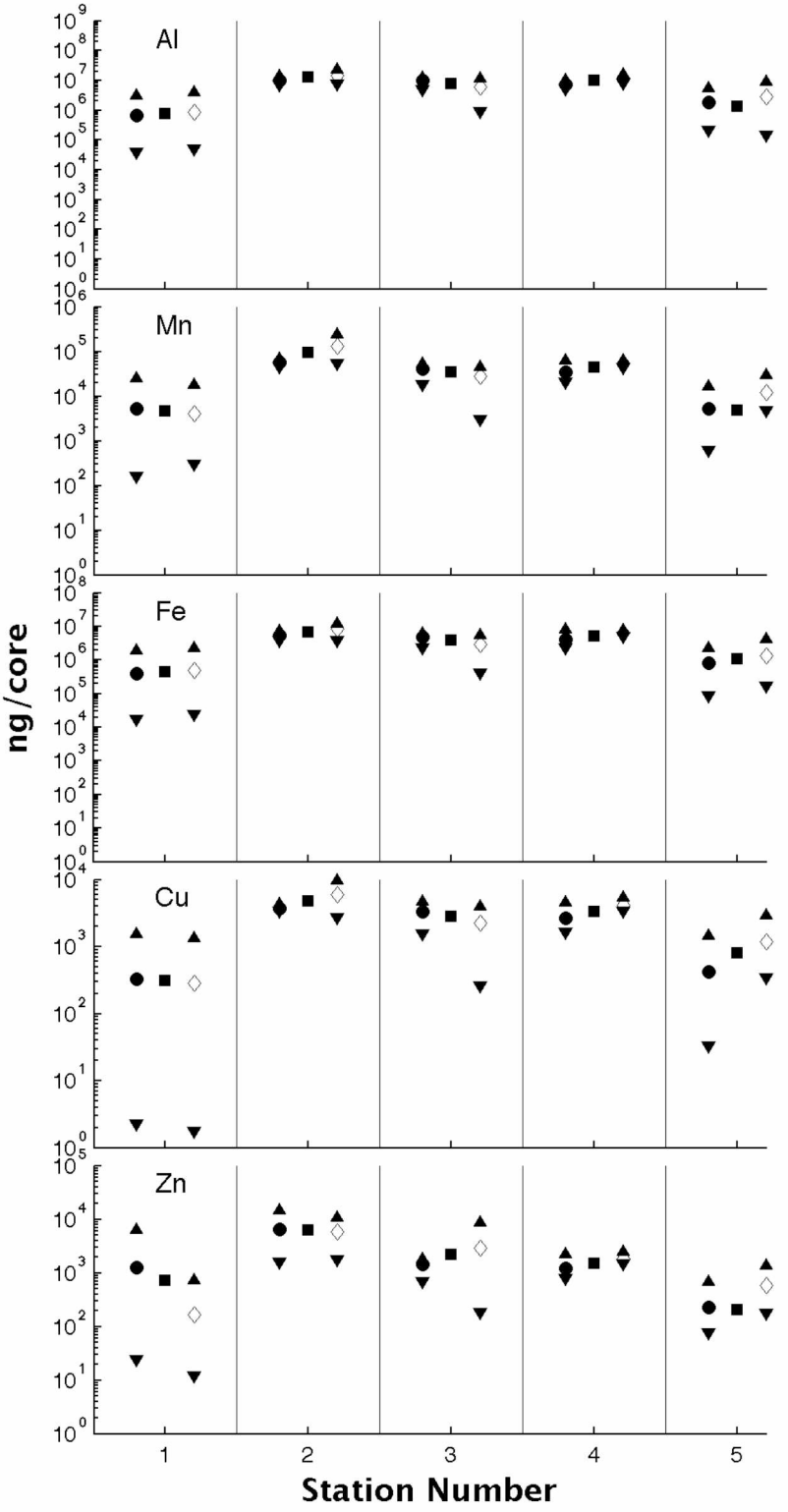

Figure 7: Average concentration (ng/core) of total particulate trace metals in the 5 grouped cores (filled squares), 5 random cores (unfilled diamond) and the average of all 10 cores (filled circle) at each station. Upward pointing triangles are the maximum concentration of an area and downward pointing triangles are the minimum.

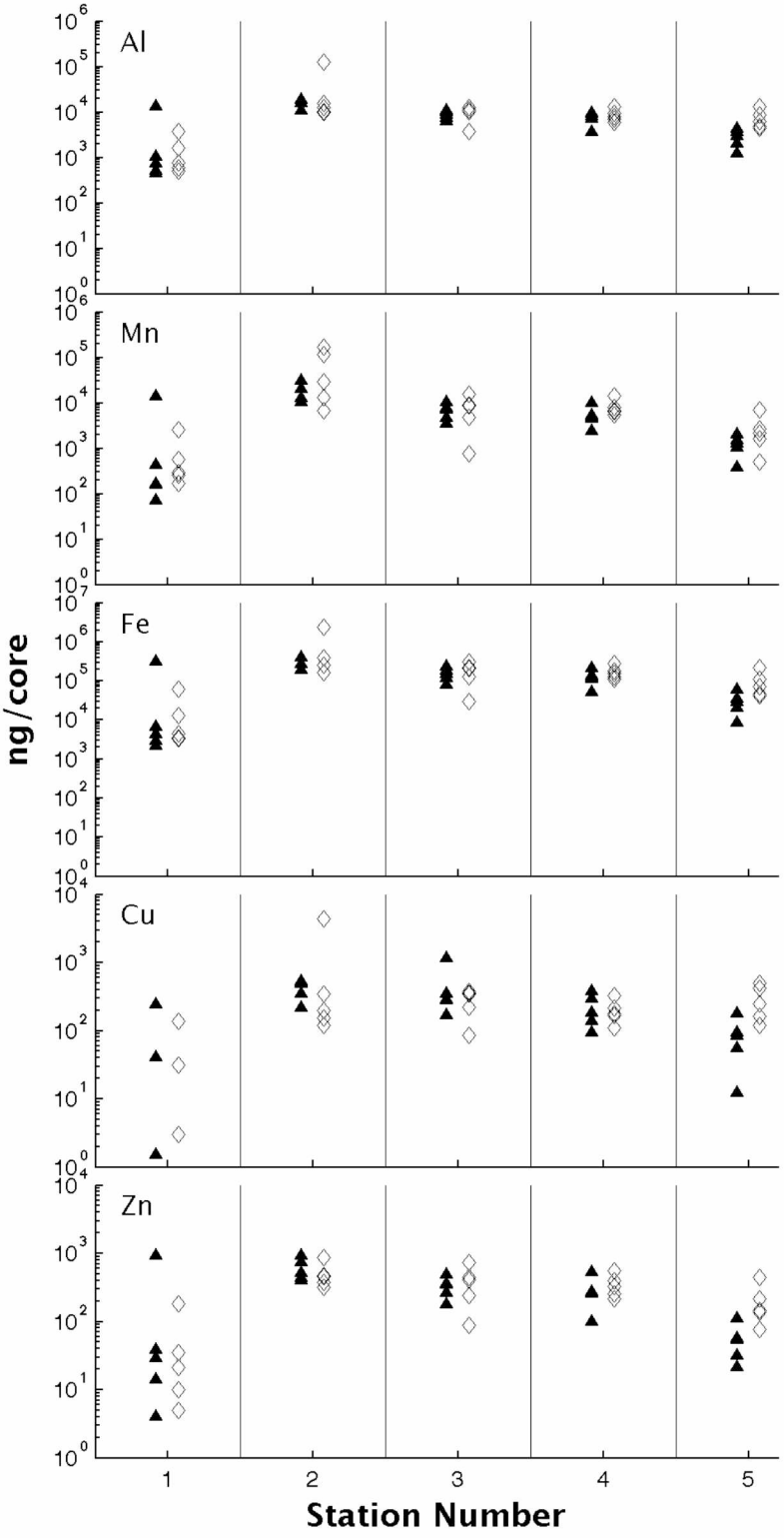

Figure 8: Range of concentrations (ng/core) of labile particulate trace elements per ice core by station. (Filled triangle: grouped cores; unfilled diamond: random cores). LPCu grouped and random cores at Station 1 had two cores with non-detectable values.

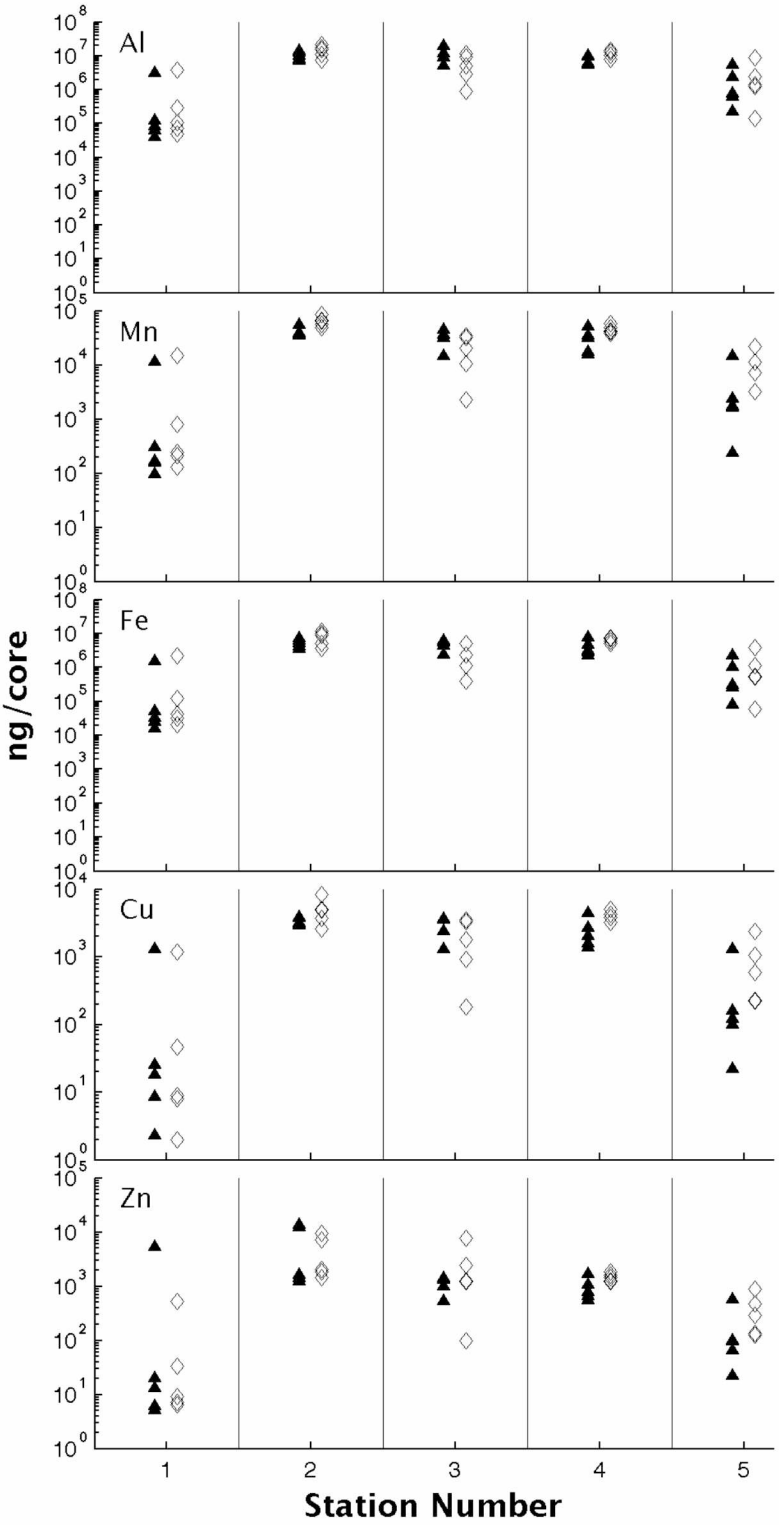

Figure 9: Range of concentrations (ng/core) of refractory particulate trace elements per ice core by station. (Filled triangle: grouped cores; unfilled diamond: random cores).

2.5 Discussion

A conceptual model of the trace element reservoirs and cycling in the sea ice environment is given in Figure 10. Trace metals are incorporated into sea ice during formation directly from the water column (Hassler and Schoemann, 2009; Lannuzel et al., 2014), by adhesion of suspended and seafloor particles into the ice matrix due to frazil ice formation on particles, by the scraping of sea ice across the seafloor (Nurnberg et al., 1994), and by the addition of atmospheric deposition, as snow or dry deposition, on top of the sea ice (Edwards and Sedwick, 2001). Percolation transfers particles and dissolved constituents between the bottom of the ice (basal ice) and underlying seawater. Ice continues to grow downward during the freezing season accumulating more particles and dissolved constituents in multiple layers, with the most biological particles typically found in the basal ice (Arrigo et al., 2009) and entrained sediment found in well-defined layers throughout the ice column (Eicken et al., 2005). Heterogeneous incorporation of particles in sea ice is further enhanced by the ridging of ice floes onto one another, creating unexpected sediment layers. The partitioning of trace metals between the dissolved and particulate phases are likely impacted by biological and abiotic processes within brine inclusions of the sea ice matrix as ice continues to grow through the winter and early spring. As the season progresses, the increase in solar radiation causes snow and ice to begin to melt, and the transfer of trace elements and other constituents from the sea ice environment to the surface of the water column (e.g., Measures, 1999; van der Merwe et al., 2011). When sea ice becomes permeable (Cox and Weeks, 1983; Golden et al., 1998) brine, which contains the majority of dissolved metals, is released from the sea ice (van der Merwe et al., 2011). The bulk of the particulate trace metals are released at a later time, as the ice matrix melts, releasing trapped particles (van der Merwe et al., 2011). Melted snow can accumulate on top of the sea ice forming melt ponds, which can drain into the sea ice brine channels and ultimately to the underlying water column (Eicken et al., 2002).

Conditions during our sampling included uneven snow cover (0 to 60 cm) likely due to snow drifting during the winter months and the storm that occurred prior to our sampling. It is likely desalination via brine drainage had already occurred prior to sampling, because the warm sea ice temperatures (- 1 °C) and low bulk salinities (2.0 to 5.1) observed indicate a permeable

sea ice regime (brine volume > 5%), enhancing the probability of loss of dissolved trace metal loads. This is supported by unexpectedly low bulk dissolved metal concentrations (Figure 6)

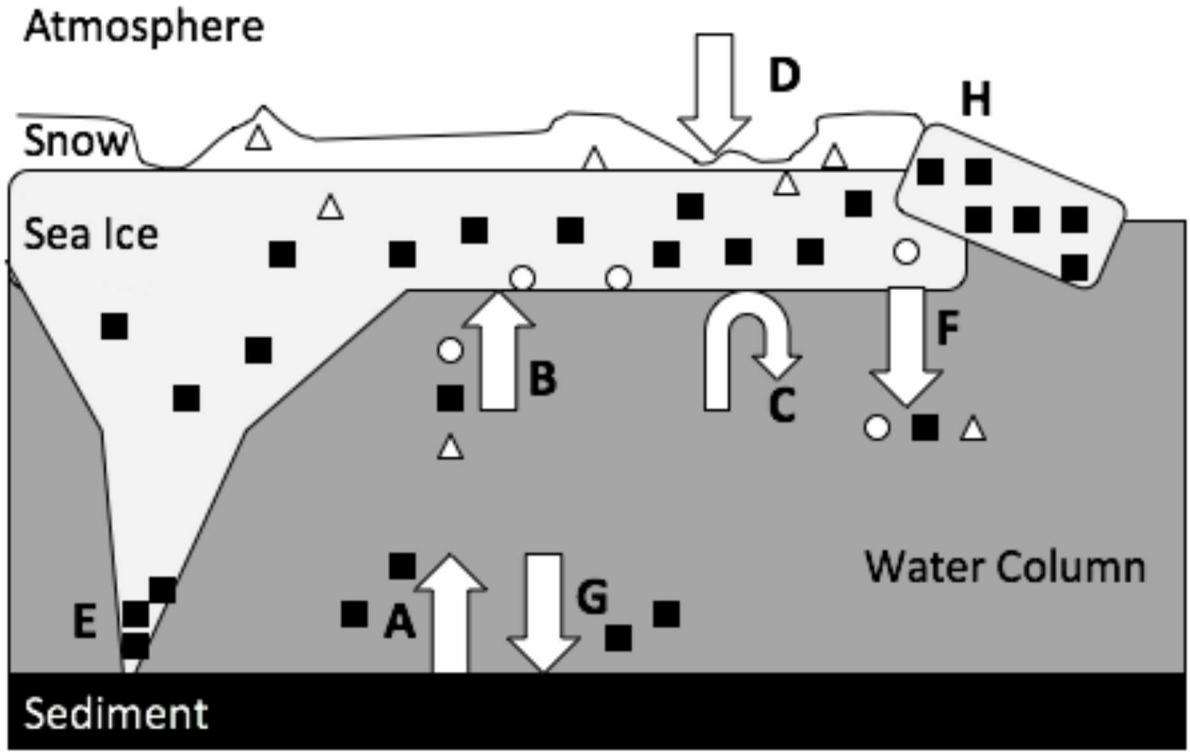

Figure 10: Conceptual model of trace metal cycling in a shallow sea ice environment. Circles represent biological particles, triangles represent atmospheric deposition and squares represent sediment. A) Resuspension or frazil ice and flotation of particles toward the surface. B) Sea ice incorporation of particles directly from the water column. C) Exchange at ice/water interface. D) Atmospheric deposition E) Sediment incorporation from the keel of sea ice scraping the sea floor. F) Release of trace metals during melt season. G) Sedimentation of particles. H) Ice floe interactions, such as the rafting of ice onto another ice sheet depicted here can potentially supply unexpected particle layers. Other floe-floe interactions not shown.

despite high sediment loads and high concentrations of particulate metals (Figure 7). We also observed a highly variable particle load in areas of jumbled ice, as well as in areas with no evident ridging. It is probable that the variability of the particle load was enhanced by fall storms that caused resuspension of sediment and ridging throughout the sampling region. Lastly, this area is known to be impacted by the Colville River. However, during our sampling Colville River outflow had not yet reached its peak (Figure 5), and river water was not apparent in the sampled sites.

2.5.1 Contribution of dissolved metals to reactive metal pools

Proximity of continental sources results in coastal waters having high concentrations of reactive particulate Fe species, which can overwhelm dFe concentrations and become the major contributor to the reactive Fe pool (de Baar and de Jong, 2001; Berger et al., 2008; Lippiatt et al., 2010; Aguilar-Islas et al., 2013). Here, we report reactive metal pools in snow and the water column as TdMetals (which includes the dissolved fraction, and the fraction of particulate metals that is solubilized at pH < 2 in a month), and in sea ice as the sum of dMetals + LPMetals (particulate metals solubilized in a hot reducing acetic acid solution). We will consider these reactive pools broadly analogous although analytical comparison of these two operationally defined pools was not carried out. We observed in our study region reactive particulate Fe to be greatly in excess of dissolved Fe throughout the water column, as well as in the snow and the sea ice (Tables 3 and 4). The highly variable particle load within the sea ice matrix resulted in reactive Fe concentrations in sea ice that varied by three orders of magnitude (11.1 to 10,100 nM), while reactive Fe in snow (26.8 to 109 nM) and the water column (38.6 to 712 nM) was less variable. The contribution from dFe to the reactive Fe pool in surface waters of this shallow coastal region was minimal, ranging from 2% to 7%, with the higher percent contribution at stations with lower TdFe concentrations. Presumably, dFe in surface waters includes the input from sea ice brine drainage at the onset of the melting season. Surface dFe values (~ 2 to 6 nM; Table 3) in this nearshore region were similar to surface values observed in summer over the Chukchi Shelf (~ 1 to 6 nM dFe; Aguilar-Islas, unpublished data), and the Laptev Shelf in water columns of ~ 50 to 60 m deep (~ 3 nM dFe; Klunder et al., 2012), suggesting that dFe values in near-coastal areas are within the same order of magnitude as under ice dFe values observed within the Transpolar Drift region (~ 2 nM; Klunder et al., 2012). In contrast, being much less particle reactive Cu and Zn were partitioned mainly into the dissolved fraction (Table 3).

It has been observed that when the ice column permeability increases in spring, the initial brine drainage delivers the bulk of dissolved metals to the surface water column (van der Merwe et al., 2011; Lannuzel et al., 2014), and as the melting season progresses the remaining trace metal load (mostly particles) is transferred to surface waters (van der Merwe et al., 2011). Prior to desalination events, seasonal interactions between particles and dissolved chemical species within brine pockets likely alter the partitioning between particulate and dissolved trace metals

within the ice matrix. The highly variable particle load within our sampling region resulted in highly variable reactive metal concentrations (Fe: 11.1 to 10,100 nM; Mn: 9.9 to 733 nM; Cu: 0.33 to 17.9 nM; Zn: 0.75 to 20.8 nM) that were much greater than those in snow (Fe: 26.8 to 109 nM; Cu: 0.18 to 1.97 nM; Zn: 0.92 to 3.36 nM) and the water column (Fe: 38.6 to 712 nM; Cu: 5.56 to 6.02 nM; Zn: 2.87 to 4.60 nM). The average contribution of the dissolved fraction to the reactive metal pool in sea ice were, as expected, minimal for Fe (1.3%), but substantial for Mn (64%), Cu (64%), and Zn (54%; Stations 2-5). Similarly, concentrations of reactive Fe in waters of this near coastal region were also dominated by suspended particles, whereas reactive Cu and Zn were dominated by the dCu and dZn fractions (Table 3). In snow, it is also expected that the reactive metal pool would be dominated by labile particles for Fe, and by dissolved species for Cu and Zn. Although we did not obtain dissolved metal values in our snow samples, Rember and Trefry (2004) reported dFe (1.74 ± 0.67 nM) and dCu (1.16 ± 0.40 nM) in coastal snow at a location ~ 80 km away from our sampling site. Assuming these values are fairly typical for the dissolved trace metal content of snow in the North Slope region at the end of the season, then, when using these values, the contribution from the dissolved fraction was as expected low for Fe (on average ~ 3%) and dominant for Cu (~ 60%).

A study in East Antarctica just offshore of Casey Station reported TdFe concentrations in snow collected on sea ice to be as high as 23.7 nM (Lannuzel et al., 2007), and snow from the Ross Sea was reported to have similar TdFe concentrations, with values reaching ~ 18 nM (Edwards and Sedwick, 2001). Values of TdFe obtained from our snow samples (26.6 to 109 nM) are greater than those observed in the above Antarctic studies, reflecting the greater atmospheric input of Fe in the Arctic, where proximity to Eurasia and North America land masses enhances deposition of natural and anthropogenic aerosols. Reactive Fe in sea ice from our samples was also found to be greater (LP+dFe: 11.1 to 10,100 nM) than reactive Fe previously measured in Southern Ocean fast ice (1.2 to 4,240 nM) (Lannuzel et al., 2016) and Southern Ocean pack ice (2.3 to 97.8 nM) (Lannuzel et al., 2016). This difference is driven by the leachable particulate fraction, as concentrations of dFe in our samples (0.40 to 3.2 nM) were within or lower than the range found in land-fast ice (1.07 to 109 nM dFe) and pack ice (0.2 to 36.8 nM) from the Southern Ocean (Lannuzel et al., 2016). However, it is worth noting that for our samples collection after desalination likely resulted in lower bulk sea ice dFe values. Sea ice

that forms over the shallower Arctic shelves has a greater potential to incorporate sediment, and thus a greater potential for supporting higher reactive Fe pools as compared to coastal sea ice formed over deeper Antarctic shelves. In contrast, elevated dFe concentrations have been observed over the shallow Bering Sea shelf in early spring prior to desalination (2.92 to 376 nM; Aguilar-Islas et al., 2008).

For trace metals other than Fe, fewer sea ice values are available in the literature. A study from Baffin Bay reported values for TdMetals and dMetals from one sea ice sample collected in the late summer of 1977 (Campbell and Yates, 1982). The reactive metal values (26.05 nM TdMn; 453 nM TdFe; and 129 nM TdCu) reported by Campbell and Yates (1982) were in the same order of magnitude for Fe and Mn as our samples (64.3 ± 32.6 nM TdMn; 746 ± 1426 nM TdFe), but our samples were lower for Cu (2.3 ± 2.5 nM TdCu). However, similarly to our observations, the contribution of the dissolved fraction to the reactive sea ice trace metal pool was low for Fe (8%) as compared to those of Mn (66%) and Cu (71%). A recent study from the East Antarctic sector of the Southern Ocean described dissolved and particulate concentrations of several trace elements in sea ice and found dAl to be correlated with bulk sea ice salinity, but correlation with bulk sea ice salinity was not found for dMn, dCu, and dZn (Lannuzel et al., 2011). This suggests that *in situ* biological and abiotic interactions between particulate and dissolved phases can alter the partitioning of micronutrients. Similarly, to Lannuzel et al. (2011), in this study the concentrations of dMn, dFe, dCu, and dZn did not correlate with sea ice salinity. However, this is not unexpected because melting whole cores likely erased any correlation between dissolved metal concentrations and sea ice salinity.

2.5.2 Variability in the sea ice particle load

We observed a wide range of sediment inclusions (~ 1 – 175 mg L^{-1}) within and among station ice cores. This wide range is expected, as sea ice sediment inclusions in the Arctic can range from zero to a few mg per liter in "clean" ice layers, to extreme concentrations greater than 3000 mg L^{-1} in heavily "dirty" ice layers, with most "turbid" sea ice layers containing a range of ~ 50 – 500 mg L^{-1} of sediment (Dethleff and Kuhlmann, 2010 and references therein). In general, most sediment inclusions within ice that formed over shelves are observed in the upper layers of the ice column (Dethleff and Kuhlmann, 2010; Wegner et al., 2017). This is because sediment

entrainment processes are most effective during autumn freeze-up events at depths shallower than ~ 50 m (Reimnitz et al., 1992; Eicken et al., 2005; Wegner et al., 2005; Sherwood 2000). However, Eicken et al. (2005) observed sediment layers throughout the ice column in sea ice from the Chukchi and western Beaufort Sea, and attributed this observation to floe-floe interactions such as rafting of sediment-laden ice floes, and/or other ice deformation events. Sediment transport by dirty sea ice formed in near-shore regions of the Beaufort Sea could be an important mechanism for transporting particles from the shelf into the deeper basin (e.g., Kempema et al., 1989; Eicken et al., 2005), including particulate carbon and trace metals from terrigenous material. From the fifty 1 m ice cores collected during this study in May, 2015, we estimated an average sea ice sediment load of 25 t/km^2 (range: 1.1 to 123 t/km^2) for eastern Beaufort fast ice, assuming our study region is representative of Beaufort Shelf. This estimate is lower than the 128 t/km^2 (range: 69 to 203 t/km^2) of sediment that can be transported by sea ice formed over the Chukchi Sea and western Beaufort Sea put forth by Eicken et al. (2005). This higher estimate was derived from 12 sediment-laden ice cores collected in 2002 and containing on average 342 mg L^{-1} of sediment. Because we did not sample the entire ice column at all stations (see Table 2), our estimate provides a lower limit in the amount of sediment incorporated into eastern Beaufort Shelf fast ice. It is possible sea ice that forms and traverses over the broad Chukchi Sea shelf has the potential to entrain a larger sediment loads than sea ice formed over the narrower Beaufort Sea shelf, but further data are needed to confirm if there is a regional distinction in sea ice sediment inventories. It is also possible that collection year was a factor in sediment inventory differences between Eicken et al. (2005) observations and our observations, Although, it has been argued that Arctic storms are intensifying (e.g., Serreze et al., 2000), which would have likely increased sediment loads in the sea ice collected in 2015. Indeed, when comparing sustained wind events greater than 10 m/s over the Chukchi and Beaufort shelves during Autumn of these two years, 2015 was a 'stormier' year (Vladimir Alexeev, pers. comm.).

Fast ice in the area we sampled is unlikely to be transported into deeper waters because Colville River water floods the surface of fast ice and a buoyant under-ice river water plume work in unison to accelerate melting (Kasper and Weingartner, 2015). This under and over ice melting results in complete ice melt in about a month after break up (Kasper and Weingartner, 2015), releasing the ice sediment load in the vicinity of the area of initial formation. In contrast,

other coastal Beaufort Sea sea ice may transport sediment hundreds of kilometers along the Beaufort shelf. For example, Darby et al. (2003) reported that ice collected ~ 22 km northwest of our sample region had entrained sediment almost exclusively from Banks Island, which is located north of the Mackenzie River, over 500 km east of their collection site. Using $^{87}Rb/^{86}Sr$ – $^{87}Sr/^{86}Sr$ isotope analysis Asahara et al. (2012) found sediment from Banks Island as far west as the Chukchi Sea, likely transported by sea ice that formed near Banks Island and melted over the Chukchi shelf.

We estimated the amount of particulate metals released to the water column from sediment inclusions, but the values reported here provide a lower limit estimate since they represent only particles found within the top 1 m of the ice column. The average particulate metal concentration/km^2 of sea ice for our region of study are 21 ± 18 kg/km^2 for TPAl, 134 ± 159 g/km^2 for TPMn, 13 ± 11 kg/km^2 for TPFe, 8.7 ± 7.7 g/km^2 for TPCu, and 7.9 ± 11.4 g/km^2 for TPZn. The amount of particulate metals that are released from sea ice can potentially have a strong impact on the reactive metal concentrations of the water column and surface sediment. However, in our region of study, it is likely most released sea ice particles would reach the seafloor prior to experiencing considerable exchange with dissolved phase in the water column, given that particles were mostly in the silt size class (0.002 mm to 0.05 mm), and would sink through 10 m of water in about 3.6 hours based on Stoke's law.

Variability in sediment inclusions was evident even within a single station (Table 5). Generally, particulate trace metals concentrations were positively correlated to sediment mass. However, it is important to note that large organic particles, such as twigs and other terrestrial plant debris were present in some samples and contributed to sediment mass. Scatter plots of TPMetal vs. TPAl (Figure 11) show that entrained sediment in our samples generally had metal to Al ratios similar to crustal ratios, which suggests lithogenic origin (Schropp et al., 1990; Lannuzel, 2014). The metal to Al ratios in sea ice entrained sediment were similar to those of Colville River Delta sediment samples, with the exception of Zn (Table 8) (Trefry et al., 2003), suggesting that the sediment entrained by the fast ice in this region originates from the Colville River. Decoupled exchange of metals between particles and dissolved phases in coastal waters prior to sea ice formation, or in brine pockets after sediment entrainment into sea ice might be

responsible for the observed variation in metal to Al ratios. Additionally, entrainment of particles other than Colville River Delta sediment may explain variations in metal ratios (e.g. Figure 11d).

Table 8: Metal to Al ratios. Values include sediment in Beaufort Sea fast ice cores, sediment from the Colville River Delta, and average metal to Al ratio from sediments collected across the globe.

Samples	Mn/Al	Fe/Al	Cu/Al	Zn/Al
Ice core sediment[1]	39.8	0.52	3.63	5.67 (0.9)
Colville River Delta[2]	50	0.49	5.8	20.5
Crustal average[3]	68.1	0.40	1.85	6.71

Al and Fe units are in g/100g of sediment, while Mn, Cu and Zn units are in µg/g of sediment; Both Zn to Al observed ratios are included. [1]This study, [2](Trefry et al., 2004), [3](Wedepohl, 1995)

2.5.3 Percent leachable metal fractions

The labile fraction of particulate metals can exchange into the dissolved phase in seasonal time scales and contribute to metals available for biological processes. We observed relatively low percent leachable metal fractions (LPMetal/ TPMetal*100%) in our sea ice entrained particles, as compared to those in other marine studies (Table 9) that determined the leachable metal fractions using the same methodology (Berger et al., 2008). The lower percent leachable

Table 9: Average Percent Leachable Metal Fractions of Particles from Various Studies.

Type of sample	Al	Mn	Fe	Cu	Zn
Landfast ice[1]	0.43% ± 0.86%	30.5% ± 18.1%	7.7% ± 9.9%	18.8% ± 15.7%	32.2% ± 20.44%
Bering Sea seawater[2]			20%		91%
Coastal Or/Wa seawater[3]	3.2 to 13.4%	62.4 to 95.7%	22.5 to 36.7%		
Bering Sea shelf water[4]	48%	96 %	79%		
Glacial Melt plume[5]	11%		11%		
Canada Basin seawater[6]			25%		
Landfast ice Barrow, AK[7]			~ 75%		

[1]This study, [2]Hurst and Bruland, 2007, [3]Berger et al., 2008, [4]Hurst et al., 2010, [5]Lippiat et al., 2010, [6]Aguilar-Islas et al., 2013, [7]Taylor, 2015

metal fraction in our samples can be an intrinsic characteristic of the particles entrained in our sea ice samples. Alternatively, it is possible that a procedural artifact resulted in the low observed leachable metal fractions. Our process required the complete melting of the 1 m ice core prior to filtration. This process took 8 to 12 hours to complete, and it is possible that labile phases were leached inside the melting chamber prior to filtration. However, this seems unlikely, as dissolved metal concentrations were not elevated, and in fact, dissolved concentrations were lower than expected given the large sediment inclusions. A more plausible explanation is that particles were leached *in situ* during winter and early spring, and elevated metal concentrations were not found in the dissolved phase due to removal of brines by desalination prior to our sampling. Lower concentrations of dFe and dMn in sea ice have been observed immediately after a desalination event (Lannuzel et al., 2014).

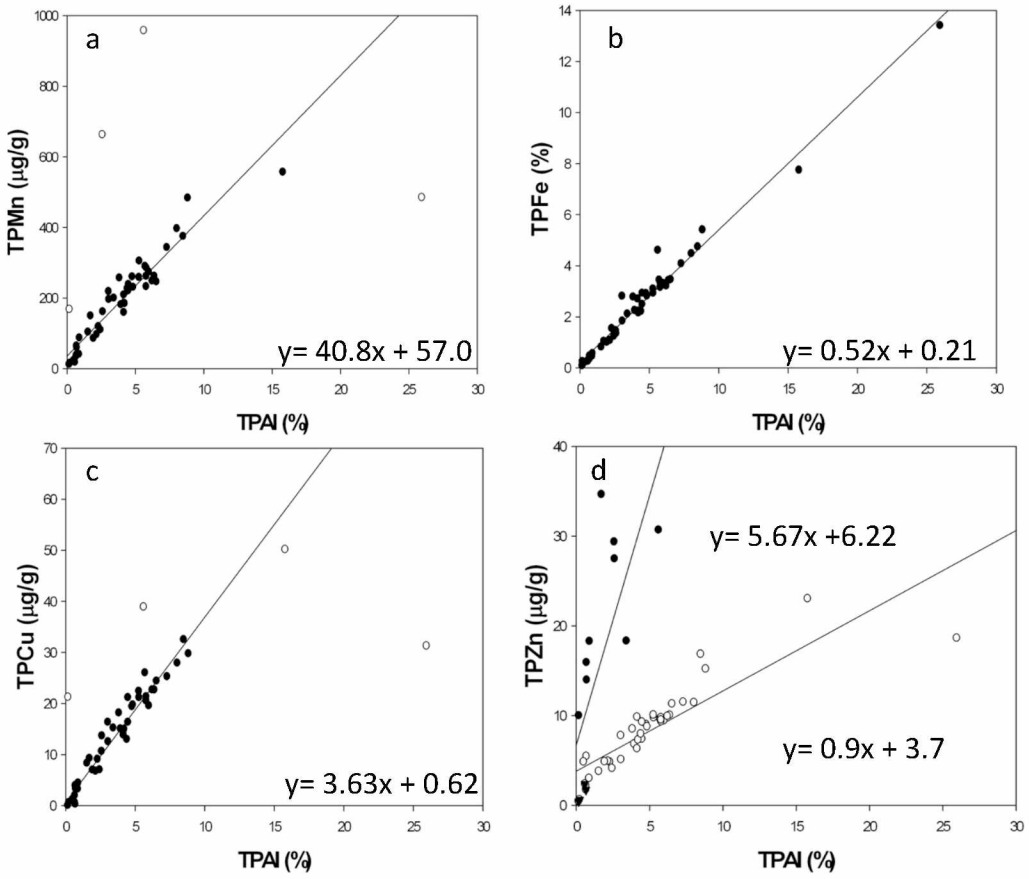

Figure 11: Scatter plots of metal to Al ratios. Unfilled points were not included in regression line calculations. These samples likely contained large organic debris. Ratios for TPZn to TPAl exhibited groupings with two distinct ratios. (Fig.11d).

2.6 Conclusions

A trace metal clean ice corer and processing equipment were developed as part of this project. We have shown that this custom-made equipment performed well, and eliminated virtually all contamination, besides the possible contamination of dZn in Station 1 when the corer was first used.

Low concentrations of dissolved metals given the large particle loads along with low percent leachable metal fractions suggest reactive metals had been released from the sea ice matrix prior to sampling. This was due to a combination of *in situ* leaching during the winter/early spring, and removal via desalination events in late spring once the ice had become permeable. Spatial variability in dissolved and particulate trace metal concentrations was found to be significant at the kilometer scale (inter-station), but not at the meter scale (intra-station). These observations have implications for future sea ice sampling studies. To assess spatial variability in trace metal content, we recommend sampling greater number of stations separated in space, and collecting fewer cores (2-3) within a given station. We also recommend temporal studies are carried out that include early and late spring sampling to determine the evolution in the release of trace metal concentrations to the underlying water column.

2.7 References

Aguilar-Islas, A.M., Rember, R.D., Mordy, C.W., Wu, J., 2008. Sea ice-derived dissolved iron and its potential influence on the spring algal bloom in the Bering Sea. Geophys. Res. Lett. 35, L24601. doi:10.1029/2008GL035736

Aguilar-Islas, A.M., Rember, R., Nishino, S., Kikuchi, T., Itoh, M., 2013. Partitioning and lateral transport of iron to the Canada Basin. Polar Sci. 7, 82–99. doi:10.1016/j.polar.2012.11.001

Arrigo, K.R., Mock, T., Lizotte, M.P., 2009. Primary Producers and Sea Ice, in: Thomas, D.S., Dieckmann, G.S. (Eds.), Sea Ice. Wiley-Blackwell, Oxford, UK, pp. 283–325. doi:10.1002/9781444317145.ch8

Asahara, Y., Takeuchi, F., Nagashima, K., Harada, N., Yamamoto, K., Oguri, K., Tadai, O., 2012. Provenance of terrigenous detritus of the surface sediments in the Bering and Chukchi Seas as derived from Sr and Nd isotopes: Implications for recent climate change in the Arctic regions. Deep Res. Part II Top. Stud. Oceanogr. 61–64, 155–171. doi:10.1016/j.dsr2.2011.12.004

Berger, C.J.M., Lippiatt, S.M., Lawrence, M.G., Bruland, K.W., 2008. Application of a chemical leach technique for estimating labile particulate aluminum, iron, and manganese in the Columbia River plume and coastal waters off Oregon and Washington. J. Geophys. Res. 113, C00B01. doi:10.1029/2007JC004703

Campbell, J.A., Yeats, P.A., 1982. The distribution of manganese , iron , nickel , copper and cadmium in the waters of Baffin Bay and the Canadian Arctic Archipelago. Oceanol. Acta 5, 161–168.

Cid, A.P., Nakatsuka, S., Sohrin, Y., 2012. Stoichiometry among bioactive trace metals in the Chukchi and Beaufort Seas. J. Oceanogr. 68, 985–1001. doi:10.1007/s10872-012-0150-8

Cox, G.F.N., Weeks, W.F., 1983. Equations for Determining the Gas and Brine Volumes in Sea-Ice Samples. J. Glaciol. 29, 306–316. doi:10.1017/S0022143000008364

Darby, D.A., 2003. Sources of sediment found in sea ice from the western Arctic Ocean, new insights into processes of entrainment and drift patterns. J. Geophys. Res. 108, 3257. doi:10.1029/2002JC001350

Darby, D.A., Myers, W.B., Jakobsson, M., Rigor, I., 2011. Modern dirty sea ice characteristics and sources: The role of anchor ice. J. Geophys. Res. 116, C09008. doi:10.1029/2010JC006675

de Baar, H.J.W., de Jong, J.T.M., 2001. Distributions, sources and sinks of iron in seawater, in: Hunter, K.A., Turner, D.R. (Eds.), The Biogeochemistry of Iron in Seawater. Wiley, West Sussex, England, pp. 123–253.

Dethleff, D., Kuhlmann, G., 2010. Fram Strait sea-ice sediment provinces based on silt and clay compositions identify Siberian Kara and Laptev seas as main source regions. Polar Res. 29, 265–282. doi:10.3402/polar.v29i3.6070

Edwards, R., Sedwick, P., 2001. Iron in east Antarctic snow: Implications for atmospheric iron deposition and algal production in Antarctic waters. Geophys. Res. Lett. 28, 3907–3910. doi:10.1029/2001GL012867

Eicken, H., Krouse, H.R., Kadko, D., Perovich, D.K., 2002. Tracer studies of pathways and rates of meltwater transport through Arctic summer sea ice. J. Geophys. Res. 107, 8046. doi:10.1029/2000JC000583

Eicken, H., Gradinger, R., Gaylord, A., Mahoney, A., Rigor, I., Melling, H., 2005. Sediment transport by sea ice in the Chukchi and Beaufort Seas: Increasing importance due to changing ice conditions? Deep Sea Res. Part II Top. Stud. Oceanogr. 52, 3281–3302. doi:10.1016/j.dsr2.2005.10.006

Golden, K.M., Ackley, S.F., Lytle, V.I., 1998. The Percolation Phase Transition in Sea Ice. Science. 282, 2238–2242.

Granskog, M.A., Virkanen, J., 2001. Observations on sea ice and surface water geochemistry-implications for the importance of sea ice in geochemical cycles in the northern Baltic Sea. Ann. Glaciol. 33, 311–316.

Hassler, C.S., Schoemann, V., 2009. Bioavailability of organically bound Fe to model phytoplankton of the Southern Ocean. Biogeosciences 6, 1677–1712. doi:10.5194/bgd-6-1677-2009

Holemann, J.A., Schirmacher, M., Kassens, H., Prange, A., 1999. Geochemistry of surficial and ice-rafted sediments from the Laptev Sea (Siberia). Estuar. Coast. Shelf Sci. 49, 45–59. doi:10.1006/ecss.1999.0485

Hurst, M.P., Bruland, K.W., 2007. An investigation into the exchange of iron and zinc between soluble, colloidal, and particulate size-fractions in shelf waters using low-abundance isotopes as tracers in shipboard incubation experiments. Mar. Chem. 103, 211–226. doi:10.1016/j.marchem.2006.07.001

Hurst, M.P., Aguilar-Islas, A.M., Bruland, K.W., 2010. Iron in the southeastern Bering Sea: Elevated leachable particulate Fe in shelf bottom waters as an important source for surface waters. Cont. Shelf Res. 30, 467–480. doi:10.1016/j.csr.2010.01.001

Kanna, N., Toyota, T., Nishioka, J., 2014. Iron and macro-nutrient concentrations in sea ice and their impact on the nutritional status of surface waters in the southern Okhotsk Sea. Prog. Oceanogr. 126, 44–57. doi:10.1016/j.pocean.2014.04.012

Kasper, J.L., Weingartner, T.J., 2015. The Spreading of a Buoyant Plume Beneath a Landfast Ice Cover. J. Phys. Oceanogr. 45, 478–494. doi:10.1175/JPO-D-14-0101.1

Kempema, E.W., Reimnitz, E., Barnes, P.W., 1989. Sea Ice Sediment Entrainment and Rafting in the Arctic. J. Sediment. Petrol. Vol. 59, 308–317. doi:10.1306/212F8F80-2B24-11D7-8648000102C1865D

Klunder, M.B., Bauch, D., Laan, P., de Baar, H.J.W., van Heuven, S., Ober, S., 2012. Dissolved iron in the Arctic shelf seas and surface waters of the central Arctic Ocean: Impact of Arctic river water and ice-melt. J. Geophys. Res. 117, C01027. doi:10.1029/2011JC007133

Lagerstrom, M.E., Field, M.P., Seguret, M., Fischer, L., Hann, S., Sherrell, R.M., 2013. Automated on-line flow-injection ICP-MS determination of trace metals (Mn, Fe, Co, Ni, Cu and Zn) in open ocean seawater: Application to the GEOTRACES program. Mar. Chem. 155, 71–80. doi:10.1016/j.marchem.2013.06.001

Lannuzel, D., Schoemann, V., de Jong, J., Tison, J.L., Chou, L., 2007. Distribution and biogeochemical behaviour of iron in the East Antarctic sea ice. Mar. Chem. 106, 18–32. doi:10.1016/j.marchem.2006.06.010

Lannuzel, D., Bowie, A.R., van der Merwe, P.C., Townsend, A.T., Schoemann, V., 2011. Distribution of dissolved and particulate metals in Antarctic sea ice. Mar. Chem. 124, 134–146. doi:10.1016/j.marchem.2011.01.004

Lannuzel, D., van der Merwe, P.C., Townsend, A.T., Bowie, A.R., 2014. Size fractionation of iron, manganese and aluminium in Antarctic fast ice reveals a lithogenic origin and low iron solubility. Mar. Chem. 161, 47–56. doi:10.1016/j.marchem.2014.02.006

Lannuzel, D., Vancoppenolle, M., van der Merwe, P., de Jong, J., Meiners, K.M., Grotti, M., Nishioka, J., Schoemann, V., 2016. Iron in sea ice: Review and new insights. Elem. Sci. Anthr. 4, 130. doi:10.12952/journal.elementa.000130

Lippiatt, S.M., Lohan, M.C., Bruland, K.W., 2010. The distribution of reactive iron in northern Gulf of Alaska coastal waters. Mar. Chem. 121, 187–199. doi:10.1016/j.marchem.2010.04.007

Measures, C.I., 1999. The role of entrained sediments in sea ice in the distribution of aluminium and iron in the surface waters of the Arctic Ocean. Mar. Chem. 68, 59–70. doi:10.1016/S0304-4203(99)00065-1

Nurnberg, D., Wollenburg, I., Dethleff, D., Eicken, H., Kassens, H., Letzig, T., Reimnitz, E., Thiede, J., 1994. Sediments in Arctic sea ice: Implications for entrainment, transport and release. Mar. Geol. 119, 185–214. doi:10.1016/0025-3227(94)90181-3

Ohnemus, D.C., Auro, M.E., Sherrell, R.M., Lagerstrom, M., Morton, P.L., Twining, B.S., Rauschenberg, S., Lam, P.J., 2014. Laboratory intercomparison of marine particulate digestions including Piranha: a novel chemical method for dissolution of polyethersulfone filters. Limnol. Oceanogr. 12, 530–547. doi:10.4319/lom.2014.12.530

Reimnitz, E., Marincovich Jr., L., McCormick, M., Briggs, W.M., 1992. Suspension freezing of bottom sediment and biota in the Northwest Passage and implications for Arctic Ocean sedimentation. Can. J. Earth Sci. 29, 693–703. doi:10.1139/e92-060

Rember, R.D., Trefry, J.H., 2004. Increased concentrations of dissolved trace metals and organic carbon during snowmelt in rivers of the alaskan arctic. Geochim. Cosmochim. Acta 68, 477–489. doi:10.1016/S0016-7037(03)00458-7

Schropp, S.J., Lewis, F.G., Windom, H.L., Ryan, J.D., Calder, F.D., Burney, L.C., 1990. Interpretation of Metal Concentrations in Estuarine Sediments of Florida Using Aluminum as a Reference Element. Estuaries 13, 227–235. doi:10.2307/1351913

Serreze, M.C., Walsh, J.E., Chapin, F.S., Osterkamp, T., Dyurgerov, M., Romanovsky, V., Oechel, W.C., Morison, J., Zhang, T., Barry, R.G., 2000. Observational Evidence of Recent Change in the Northern High-Latitude Environment. Clim. Change 46, 159–207. doi:10.1023/A:1005504031923

Sherwood, C.R., 2000. Numerical model of frazil ice and suspended sediment concentrations and formation of sediment laden ice in the Kara Sea. J. Geophys. Res. 105, 14061–14080. doi:10.1029/2000JC900037

Taylor, M.A., 2015. High concentrations of potentially bioavailable iron on Arctic sea ice particles [dissertation]. University of Michigan.

Tovar-Sánchez, A., Duarte, C.M., Alonso, J.C., Lacorte, S., Tauler, R., Galban-Malagón, C., 2010. Impacts of metals and nutrients released from melting multiyear Arctic sea ice. J. Geophys. Res. C Ocean. 115, C07003. doi:10.1029/2009JC005685

Trefry, J.H., Rember, R.D., Trocine, R.P., Brown, J.S., 2003. Trace metals in sediments near offshore oil exploration and production sites in the Alaskan Arctic. Environ. Geol. 45, 149–160. doi:10.1007/s00254-003-0882-2

van der Merwe, P., Lannuzel, D., Bowie, A.R., Mancuso Nichols, C.A., Meiners, K.M., 2011. Iron fractionation in pack and fast ice in East Antarctica: Temporal decoupling between the release of dissolved and particulate iron during spring melt. Deep Res. Part II Top. Stud. Oceanogr. 58, 1222–1236. doi:10.1016/j.dsr2.2010.10.036

Vancoppenolle, M., Meiners, K.M., Michel, C., Bopp, L., Brabant, F., Carnat, G., Delille, B., Lannuzel, D., Madec, G., Moreau, S., Tison, J., Merwe, P. Van Der, 2013. Role of sea ice in global biogeochemical cycles : emerging views and challenges. Quat. Sci. Rev. 1–24. doi:10.1016/j.quascirev.2013.04.011

Wedepohl, K.H., 1995. The composition of the continental crust. Geochim. Cosmochim. Acta 59, 1217–1232. doi:10.1016/0016-7037(95)00038-2

Wegner, C., Hölemann, J.A., Dmitrenko, I., Kirillov, S., Kassens, H., 2005. Seasonal variations in Arctic sediment dynamics - Evidence from 1-year records in the Laptev Sea (Siberian Arctic). Glob. Planet. Change 48, 126–140. doi:10.1016/j.gloplacha.2004.12.009

Wegner, C., Wittbrodt, K., Hölemann, J.A., Janout, M.A., Krumpen, T., Selyuzhenok, V., Novikhin, A., Polyakova, Y., Krykova, I., Kassens, H., Timokhov, L., 2017. Sediment entrainment into sea ice and transport in the Transpolar Drift: A case study from the Laptev Sea in winter 2011/2012. Cont. Shelf Res. 141, 1–10. doi:10.1016/j.csr.2017.04.010

Chapter 3: Conclusions

The purpose of this thesis was to provide first time trace metal data in Arctic fast ice to contribute to the ongoing effort to better understand the Arctic ecosystem that is being impacted by changes in sea ice dynamics. The results of this study answer questions about the dynamic coastal Arctic environment that will inform future studies The custom-built trace element clean ice corer and melting chambers that were developed for this study were shown to provide clean samples and to be instrumental tools for efficient studies of trace metals in sea ice. Statistical analysis of dissolved and particulate trace metal variability in sea ice has provided information about the scale of heterogeneity for the Beaufort Sea fast ice environment that can be used to design future sampling plans. Paired with the knowledge of temporal variability that was inferred through this study and that has been previously described in Antarctic sea ice (e.g., van der Merwe et al., 2011), it is recommended that future sea ice sampling should include collection to capture the seasonal evolution of trace metal concentrations across kilometer spatial scales. The metal/Al ratios and the relatively low labile particulate metal concentrations described in Chapter 1, indicate the dominance of lithogenic particles in sampled fast ice, and suggest that these particles undergo leaching within the sea ice matrix. These observations provide process information to aid modeling efforts concerned with trace metal loads in Arctic sea ice (e.g.,Wang et al., 2014). Ultimately, with a more comprehensive understanding of the role sea ice plays in trace metal cycling in the Arctic Ocean, more accurate predictions can be made about impacts caused by further changes to the dynamics of Arctic sea ice.

3.1 Introduction and Conclusions References

Aguilar-Islas, A.M., Rember, R.D., Mordy, C.W., Wu, J., 2008. Sea ice-derived dissolved iron and its potential influence on the spring algal bloom in the Bering Sea. Geophys. Res. Lett. 35, 10–14. doi:10.1029/2008GL035736

Alekseev, G., Glok, N., Smirnov, A., 2016. On assessment of the relationship between changes of sea ice extent and climate in the Arctic. Int. J. Climatol. 36, 3407–3412. doi:10.1002/joc.4550

Arrigo, K.R., van Dijken, G., Pabi, S., 2008. Impact of a shrinking Arctic ice cover on marine primary production. Geophys. Res. Lett. 35, 1–6. doi:10.1029/2008GL035028

Arrigo, K.R., 2014. Sea Ice Ecosystems. Ann. Rev. Mar. Sci. 6, 439–467. doi:10.1146/annurev-marine-010213-135103

Bian, H., Colarco, P.R., Chin, M., Chen, G., Rodriguez, J.M., Liang, Q., Blake, D., Chu, D.A., Da Silva, A., Darmenov, A.S., Diskin, G., Fuelberg, H.E., Huey, G., Kondo, Y., Nielsen, J.E., Pan, X., Wisthaler, A., 2013. Source attributions of pollution to thewestern arctic during the nasa arctas field campaign. Atmos. Chem. Phys. 13, 4707–4721. doi:10.5194/acp-13-4707-2013

Breider, T.J., Mickley, L.J., Jacob, D.J., Wang, Q., Fisher, J.A., Chang, R.Y., Alexander, B., 2014. Journal of Geophysical Research : Atmospheres and aerosol absorption. J. Geophys. Res. Atmos. 119, 4107–4124. doi:10.1002/2013JD020996

Bullard, J.E., Baddock, M., Bradwell, T., Crusius, J., Darlington, E., Gaiero, D., Gassó, S., Gisladottir, G., Hodgkins, R., McCulloch, R., McKenna-Neuman, C., Mockford, T., Stewart, H., Thorsteinsson, T., 2016. High-latitude dust in the Earth system. Rev. Geophys. 54, 447–485. doi:10.1002/2016RG000518

Campbell, J.A., Yeats, P.A., 1982. The distribution of manganese , iron , nickel , copper and cadmium in the waters of Baffin Bay and the Canadian Arctic Archipelago. Oceanol. Acta 5, 161–168.

Comiso, J.C., Parkinson, C.L., Gersten, R., Stock, L., 2008. Accelerated decline in the Arctic sea ice cover. Geophys. Res. Lett. 35, L01703. doi:10.1029/2007GL031972

Curry, J. A., Schramm, J.L., Ebert, E.E., 1995. Sea Ice-Albedo Climate Feedback Mechanism. J. Clim. 8, 240–247. doi:10.1175/1520-0442(1995)008<0240:SIACFM>2.0.CO;2

Darby, D.A., Myers, W.B., Jakobsson, M., Rigor, I., 2011. Modern dirty sea ice characteristics and sources: The role of anchor ice. J. Geophys. Res. 116, C09008. doi:10.1029/2010JC006675

Dieckmann, G.S., Hellmer, H.H., 2009. The Importance of Sea Ice: An Overview, in: Thomas, D.N., Dieckmann, G.S. (Eds.), Sea Ice. Wiley-Blackwell, Oxford, UK, pp. 1–22. doi:10.1002/9781444317145.ch1

Eicken, H., Gradinger, R., Gaylord, A., Mahoney, A., Rigor, I., Melling, H., 2005. Sediment transport by sea ice in the Chukchi and Beaufort Seas: Increasing importance due to changing ice conditions? Deep Sea Res. Part II Top. Stud. Oceanogr. 52, 3281–3302. doi:10.1016/j.dsr2.2005.10.006

Golden, K.M., Ackley, S.F., Lytle, V.I., 1998. The Percolation Phase Transition in Sea Ice. Science. 282, 2238–2242.

Golden, K.M., Eicken, H., Heaton, A.L., Miner, J., Pringle, D.J., Zhu, J., 2007. Thermal evolution of permeability and microstructure in sea ice. Geophys. Res. Lett. 34, L16501. doi:10.1029/2007GL030447

Groot Zwaaftink, C.D., Grythe, H., Skov, H., Stohl, A., 2016. Substantial contribution of northern high-latitude sources to mineral dust in the Arctic. J. Geophys. Res. Atmos. 121, 678–697. doi:10.1002/2016JD025482

Hassler, C.S., Schoemann, V., 2009. Bioavailability of organically bound Fe to model phytoplankton of the Southern Ocean. Biogeosciences 6, 1677–1712. doi:10.5194/bgd-6-1677-2009

Hoffmann, L.J., Breitbarth, E., Boyd, P.W., Hunter, K.A., 2012. Influence of ocean warming and acidification on trace metal biogeochemistry. Mar. Ecol. Prog. Ser. 470, 191–205. doi:10.3354/meps10082

Holemann, J.A., Schirmacher, M., Kassens, H., Prange, A., 1999. Geochemistry of surficial and ice-rafted sediments from the Laptev Sea (Siberia). Estuar. Coast. Shelf Sci. 49, 45–59. doi:10.1006/ecss.1999.0485

IPCC, 2014. IPCC, 2014: Climate Change 2014: Synthesis Report. Contribution of Working Groups I, II and III to the Fifth Assessment Report of the Intergovernmental Panel on Climate Change [Core Writing Team, R.K. Pachauri and L.A. Meyer (eds.)]. Geneva, Switzerland.

Jickells, T.D., An, Z.S., Andersen K. K., Baker, A.R., Bergametti, G., Brooks, N., Cao, J.J., Boyd, P.W., Duce, R.A., Hunter, K.A., Kawahata, H., Kubilay, N., LaRoche, J., Liss, P.S., Mahowald, N., Prospero, J.M., Ridgwell, A.J., Tegen, I., Torres, R., 2005. Global Iron Connections Between Desert Dust, Ocean Biogeochemistry, and Climate. Science. 308, 67–71. doi:10.1126/science.1105959

Kasper, J.L., Weingartner, T.J., 2015. The Spreading of a Buoyant Plume Beneath a Landfast Ice Cover. J. Phys. Oceanogr. 45, 478–494. doi:10.1175/JPO-D-14-0101.1

Klunder, M.B., Bauch, D., Laan, P., de Baar, H.J.W., van Heuven, S., Ober, S., 2012. Dissolved iron in the Arctic shelf seas and surface waters of the central Arctic Ocean: Impact of Arctic river water and ice-melt. J. Geophys. Res. 117, C01027. doi:10.1029/2011JC007133

Kwok, R., Rothrock, D.A., 2009. Decline in Arctic sea ice thickness from submarine and ICESat records: 1958-2008. Geophys. Res. Lett. 36, L15501. doi:10.1029/2009GL039035

Kwok, R., Cunningham, G.F., 2015. Variability of Arctic sea ice thickness and volume from CryoSat-2. Philos. Trans. R. Soc. A 373, 1–20. doi:10.1098/rsta.2014.0157

Lannuzel, D., Schoemann, V., de Jong, J., Pasquer, B., van der Merwe, P., Masson, F., Tison, J.L., Bowie, A., 2010. Distribution of dissolved iron in Antarctic sea ice: Spatial, seasonal, and inter-annual variability. J. Geophys. Res. 115, 1–13. doi:10.1029/2009JG001031

Lannuzel, D., Vancoppenolle, M., van der Merwe, P., de Jong, J., Meiners, K.M., Grotti, M., Nishioka, J., Schoemann, V., 2016. Iron in sea ice: Review and new insights. Elem. Sci. Anthr. 4, 130. doi:10.12952/journal.elementa.000130

Laxon, S.W., Giles, K.A., Ridout, A.L., Wingham, D.J., Willatt, R., Cullen, R., Kwok, R., Schweiger, A., Zhang, J., Haas, C., Hendricks, S., Krishfield, R., Kurtz, N., Farrell, S., Davidson, M., 2013. CryoSat-2 estimates of Arctic sea ice thickness and volume. Geophys. Res. Lett. 40, 732–737. doi:10.1002/grl.50193

Liu, D., Quennehen, B., Darbyshire, E., Allan, J.D., Williams, P.I., Taylor, J.W., J.-B. Bauguitte, S., Flynn, M.J., Lowe, D., Gallagher, M.W., Bower, K.N., Choularton, T.W., Coe, H., 2015. The importance of Asia as a source of black carbon to the European Arctic during springtime 2013. Atmos. Chem. Phys. 15, 11537–11555. doi:10.5194/acp-15-11537-2015

Markus, T., Stroeve, J.C., Miller, J., 2009. Recent changes in Arctic sea ice melt onset, freezeup, and melt season length. J. Geophys. Res. 114, 1–14. doi:10.1029/2009JC005436

Nurnberg, D., Wollenburg, I., Dethleff, D., Eicken, H., Kassens, H., Letzig, T., Reimnitz, E., Thiede, J., 1994. Sediments in Arctic sea ice: Implications for entrainment, transport and release. Mar. Geol. 119, 185–214. doi:10.1016/0025-3227(94)90181-3

Perovich, D.K., Richeter-Menge, J.A., Jones, K.F., Light, B., 2008. Sunlight, water, and ice: Extreme Arctic sea ice melt during the summer of 2007. Geophys. Res. Lett. 35, 2–5. doi:10.1029/2008GL034007

Perrette, M., Yool, A., Quartly, G.D., Popova, E.E., 2011. Near-ubiquity of ice-edge blooms in the Arctic. Biogeosciences 8, 515–524. doi:10.5194/bg-8-515-2011

Petrich, C., Eicken, H., 2009. Growth, Structure and Properties of Sea Ice, in: Thomas, D.N., Dieckmann, G.S. (Eds.), Sea Ice. Wiley-Blackwell, Oxford, UK, pp. 23–77. doi:10.1002/9781444317145.ch2

Popovicheva, O.B., Evangeliou, N., Eleftheriadis, K., Kalogridis, A.C., Sitnikov, N., Eckhardt, S., Stohl, A., 2017. Black Carbon Sources Constrained by Observations in the Russian High Arctic. Environ. Sci. Technol. 51, 3871–3879. doi:10.1021/acs.est.6b05832

Rampal, P., Weiss, J., Marsan, D., Bourgoin, M., 2009. Arctic sea ice velocity field: General circulation and turbulent-like fluctuations. J. Geophys. Res. Ocean. 114, C10014. doi:10.1029/2008JC005227

Richter-Menge, J., Mathis, J., 2016. The Arctic [in "State of the Climate 2015"]. Bull. Am. Meteorol. Soc. 97 (8), S131–S153.

Serreze, M.C., Walsh, J.E., Chapin, F.S., Osterkamp, T., Dyurgerov, M., Romanovsky, V., Oechel, W.C., Morison, J., Zhang, T., Barry, R.G., 2000. Observational Evidence of Recent Change in the Northern High-Latitude Environment. Clim. Change 46, 159–207. doi:10.1023/A:1005504031923

Shaw, G.E., Khalil, M.A.K., 1989. Arctic Haze, in: Air Pollution. Springer Berlin Heidelberg, Berlin, Heidelberg, pp. 69–111. doi:10.1007/978-3-540-46113-5_3

Smith, W.O., Nelson, D.M., 1985. Phytoplankton bloom produced by a receding ice edge in the Ross Sea: spatial coherence with the density field. Science. 227, 163–166. doi:10.1126/science.227.4683.163

Stroeve, J.C., Markus, T., Boisvert, L., Miller, J., Barrett, A., 2014. Changes in Arctic melt season and implifications for sea ice loss. Geophys. Res. Lett. 41, 1216–1225. doi:10.1002/2013GL058951

Taylor, M.A., 2015. High concentrations of potentially bioavailable iron on Arctic sea ice particles [dissertation]. University of Michigan.

Taylor, R.L., Semeniuk, D.M., Payne, C.D., Zhou, J., Tremblay, J.E., Cullen, J.T., Maldonado, M.T., 2013. Colimitation by light, nitrate, and iron in the Beaufort Sea in late summer. J. Geophys. Res. Ocean. 118, 3260–3277. doi:10.1002/jgrc.20244

Tovar-Sánchez, A., Duarte, C.M., Alonso, J.C., Lacorte, S., Tauler, R., Galban-Malagón, C., 2010. Impacts of metals and nutrients released from melting multiyear Arctic sea ice. J. Geophys. Res. C Ocean. 115, C07003. doi:10.1029/2009JC005685

van der Merwe, P., Lannuzel, D., Bowie, A.R., Mancuso Nichols, C.A., Meiners, K.M., 2011. Iron fractionation in pack and fast ice in East Antarctica: Temporal decoupling between the release of dissolved and particulate iron during spring melt. Deep Res. Part II Top. Stud. Oceanogr. 58, 1222–1236. doi:10.1016/j.dsr2.2010.10.036

Vancoppenolle, M., Meiners, K.M., Michel, C., Bopp, L., Brabant, F., Carnat, G., Delille, B., Lannuzel, D., Madec, G., Moreau, S., Tison, J., Merwe, P. Van Der, 2013. Role of sea ice in global biogeochemical cycles : emerging views and challenges. Quat. Sci. Rev. 1–24. doi:10.1016/j.quascirev.2013.04.011

Walsh, J.E., 2014. Intensified warming of the Arctic: Causes and impacts on middle latitudes. Glob. Planet. Change 117, 52–63. doi:10.1016/j.gloplacha.2014.03.003

Wang, S., Bailey, D., Lindsay, K., Moore, J.K., Holland, M., 2014. Impact of sea ice on the marine iron cycle and phytoplankton productivity. Biogeosciences 11, 4713–4731. doi:10.5194/bg-11-4713-2014

Wells, M.L., Priceb, N.M., Bruland, K.W., 1995. Iron chemistry in seawater and its relationship to phytoplankton : a workshop report. Mar. Chem. 48, 157–182.